energy&fuels

pubs.acs.org/EF
Article

Experimental and Modeling High-Pressure Study of Ammonia−Methane Oxidation in a Flow Reactor

Pedro García-Ruiz, Iris Salas, Eva Casanova, Rafael Bilbao, and María U. Alzueta*

Cite This: *Energy Fuels* 2024, 38, 1399−1415

ABSTRACT: The present work deals with an experimental and modeling analysis of the oxidation of ammonia−methane mixtures at high pressure (up to 40 bar) in the 550−1250 K temperature range using a quartz tubular reactor and argon as a diluent. The impact of temperature, pressure, oxygen stoichiometry, and CH_4/NH_3 ratio has been analyzed on the concentrations of NH_3, NO_2, N_2O, NO, N_2, HCN, CH_4, CO, and CO_2 obtained as main products of the ammonia−methane mixture oxidation. The main results obtained indicate that increasing either the pressure, CH_4/NH_3 ratio, or stoichiometry results in a shift of NH_3 and CH_4 conversion to lower temperatures. The effect of pressure is particularly significant in the low range of pressures studied. The main products of ammonia oxidation are N_2, NO, and N_2O while NO_2 concentrations are below the detection limit for all of the conditions considered. The N_2O formation is favored by increasing the CH_4/NH_3 ratio and stoichiometry. The experimental results are simulated and interpreted in terms of an updated detailed chemical kinetic mechanism, which, in general, is able to describe well the conversion of both NH_3 and CH_4 under almost all of the studied conditions. Nevertheless, some discrepancies are found between the experimental results and model calculations.

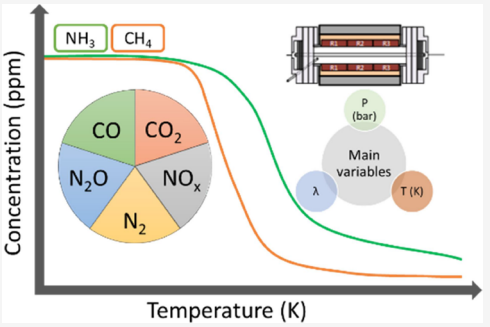

INTRODUCTION

Nowadays, the rise in the global concentration of carbon dioxide and harmful pollutants due to the growing energy demand has become a serious problem. Future sustainable scenarios involve the use of carbon-free fuels. In this sense, species such as hydrogen and ammonia play a role as possible substitutes for fossil fuels,[1] to solve the climate change problem. An alternative solution is the use of noncarbon fuels, such as ammonia or hydrogen, as fuels or as chemical storage.[2] Hydrogen has attracted attention as a fuel with zero CO_2 emissions,[3] but it has some application inconveniences associated with its high storage cost. Proof of this is the fact that storing H_2 at high scales in practical applications implies compression to between 350−700 bar or cryogenic cooling to 20 K.[4] For these reasons, H_2 storage is more difficult and expensive than storing NH_3.[5] Moreover, following the interest in ammonia as a hydrogen carrier, there is nowadays an increased interest in ammonia as a fuel. Since ammonia is one of the most produced chemicals in the world, it exhibits a mature production technology, transportation, and storage infrastructure.[6,7] Ammonia has been suggested as a substitute for hydrogen,[8] and since the previous decade, initiatives to accelerate global decarbonization have increasingly focused on the use of NH_3 as a feasible alternative fuel.[9] Additionally, ammonia can ideally be burned in an environmentally benign way, producing N_2 and H_2O (R1)[10]:

$$4NH_3 + 3O_2 \rightleftharpoons 2N_2 + 6H_2O \quad \text{(R1)}$$

At the same time, NH_3 could potentially be a future NO_x-free fuel under specific operating conditions as Shu et al.[11] conclude, since ammonia can interact under specific conditions (fuel-lean conditions) within the combustion chamber with NO, effectively minimizing its concentration through selective noncatalytic (SNCR) reactions.[10−14] In this way, ammonia can react with NO by the following mechanisms ($NH_3 \rightarrow NO \rightarrow NNH \rightarrow N_2$ and $NH_3 \rightarrow NO \rightarrow N_2$) within the combustion chamber, as pointed out by Alzueta et al.[12] through reactions (R2−R5):

$$NH_3 + OH \rightleftharpoons NH_2 + H_2O \quad \text{(R2)}$$

$$NH_2 + NO \rightleftharpoons N_2 + H_2O \quad \text{(R3)}$$

$$NH_2 + NO \rightleftharpoons NNH + OH \quad \text{(R4)}$$

$$NNH \rightleftharpoons N_2 + H \quad \text{(R5)}$$

However, ammonia presents some challenges for its practical implementation associated with its poor combustion characteristics, such as its high ignition temperature and low flammability,[7,10] potential NO_x emissions,[12] and a low laminar burning velocity which is about five times lower compared to CH_4/air flames.[15] Thus, the addition of CH_4 can improve the

Received: October 11, 2023
Revised: December 21, 2023
Accepted: December 21, 2023
Published: January 8, 2024

https://doi.org/10.1021/acs.energyfuels.3c03959
Energy Fuels 2024, 38, 1399−1415

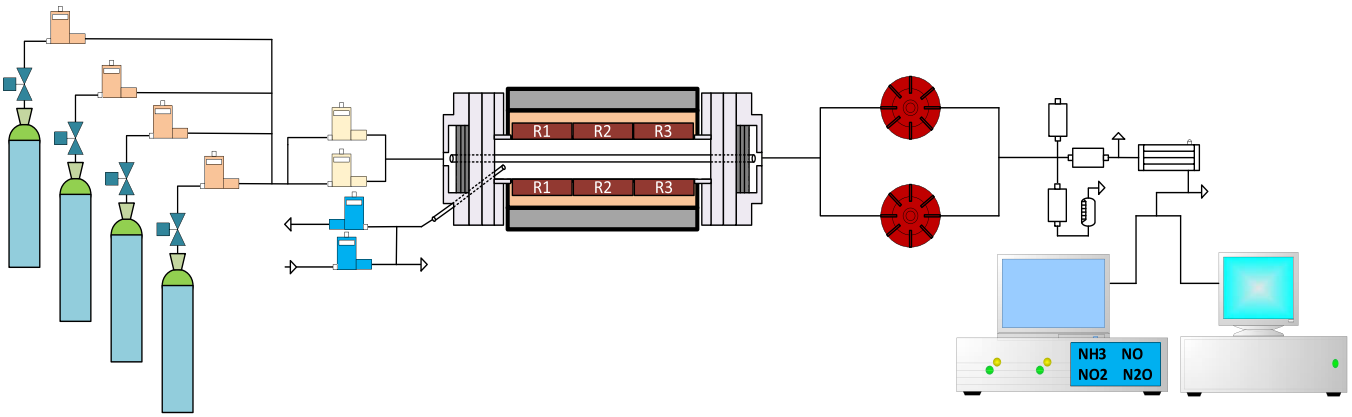

Figure 1. Laboratory-scale high-pressure setup.

combustion characteristics of ammonia,[14] because it can provide a higher flame speed, and a higher thermal efficiency[16] at the same time. The NH_3/CH_4 mixture also provides an advantage for CO_2 emissions minimization compared to natural gas burning because ammonia replaces part of the hydrocarbon fuel. Under locally fuel-rich conditions within the combustion chamber, CH_4 also can reduce the NO concentration, mainly by reburn reactions.[12] In the NH_3/CH_4 mixtures, the reburn reactions occur through the generation of hydrocarbon radicals at high temperatures and fuel-rich conditions, which are able to interact with NO, through reactions (R6,R7),[17] involving the methyl radical formed from methane (R8):

$$CH_3 + NO \rightleftharpoons HCN + H_2O \quad \text{(R6)}$$

$$CH_3 + NO \rightleftharpoons H_2CN + OH \quad \text{(R7)}$$

$$CH_4 + OH \rightleftharpoons CH_3 + H_2O \quad \text{(R8)}$$

The intermediate species HCN and H_2CN formed will be converted to N_2 or NO within the combustor chamber under specific conditions. The combined use of ammonia and methane can be beneficial for NO_x reduction through the two mechanisms described above, namely, SNCR and reburn. In the past few years, for the above reasons among others, mixtures of NH_3 with other fuels such as CH_4 have exhibited a strong interest to be accounted for in the transition from energy systems based on fossil fuels to others based on carbon-free fuels. A large number of experimental and modeling studies of the combustion of NH_3/CH_4 mixtures at low pressure (from 0.4 to 5 bar) have been reported in the literature, using different experimental set-ups such as flow reactors,[12,18−20] different burners such as the Mckenna burner,[21] a plate burner,[22] a swirl burner,[8,23,24] an axisymmetric burner,[25] a heat flux burner,[26] different premixed laminar burners,[27−29] and a porous media burner,[30] as well as combustors such as cylindrical combustor chambers,[6,16,31] turbines such as a micro gas turbine combustor,[14] a swirl flame combustor,[24,32−34] and gas turbine systems,[35−38] as well as numerical studies.[39−42]

Among the previous studies, we can find flame studies,[8,21,25] emissions characteristics, flame propagations, flame structure, autoignition properties,[14,35,39] laminar burning velocity and flame speed,[6,16,26,29] and numerical studies.[6,8,11,12,14,16,18,20−25,27−30,32,34−36,39−43]

It is important to mention as well that some studies at atmospheric pressure focused on determining the effects of NO concentration on ammonia chemistry during NH_3/CH_4 mixtures oxidation.[12,22,27,40] Also, the effects of CO/CO_2 are also studied on NH_3 oxidation in a flow reactor with the aim of addressing possible oxy-fuel combustion strategies.[18,27,44−46]

From a practical point of view, pressure is an important variable since turbines and certain engines will operate under high pressure conditions.

Increasing pressure has been reported to contribute to reduce the unburned NH_3 and NO emission.[47] In this sense, it is essential to examine whether the same effect happens for other reaction products, such as HCN. In this regard, studies in the literature on NH_3/CH_4 blends at high pressure (from 5 to 100 bar) are rather scarce, and among those we can mention a study on turbulent burning velocity and flame region in a nozzle burner at 5 bar by Ichikawa et al.,[48] an autoignition delay time study from 20 to 70 bar and temperatures from 930 to 1140 K of different CH_4/NH_3 mixtures (0, 5, 10 and 50% of CH_4 in the mixture) in a rapid compression machine by Dai et al.,[43] an experimental and numerical study of autoignition at 1.75 and 10 bar in a shock tube, in which CH_4/NH_3 ratios of 0, 0.1, and 0.5 were studied,[49] an experimental and numerical study on laminar burning velocity in a pressurized chamber up to 5 bar by Wang et al.[50] and chemical kinetic modeling studies.[34,41] In these studies, it was found that, at higher pressures, there is less unburned NH_3 and lower NO emissions at the outlet of the reactor compared to what occurs at atmospheric pressure. Additionally, the ignition delay time decreases as CH_4 is added to the mixture, even if added in a small ratio, compared to the conversion of net ammonia. The oxygen excess ratio is also important since the ignition delay time is higher at lower oxygen concentrations. Furthermore, methane has an enhancing effect on ignition due to its impact on H_2O_2, CH_3O, and H_2NO, resulting in the promoting effect of ammonia conversion under different conditions.[43,48−50]

To our knowledge, there is a lack of studies about NH_3/CH_4 mixture oxidation under relevant conditions carried out in plug flow reactors and high pressures (10 to 40 bar) in a variety of stoichiometries ranging from reducing to oxidizing atmospheres. In this context, the aim of this work is to extend the knowledge of NH_3/CH_4 mixtures oxidation using the experimental system described above, by analyzing the effect of temperature (from 550 to 1250 K), pressure (from 10 to 40 bar), oxygen excess ratio (from reducing, $\lambda = 0.7$, to oxidizing conditions, $\lambda = 3$) and CH_4/NH_3 ratio (0.5, 1 and 2). Experiments are performed using argon as a bath gas, which allows us to accurately determine the molecular nitrogen formed during the reaction and therefore to be able to perform nitrogen balances. Additionally, in order to understand the chemistry and product species formation, the

https://doi.org/10.1021/acs.energyfuels.3c03959
Energy Fuels 2024, 38, 1399−1415

results are interpreted in terms of a chemical kinetic mechanism for ammonia/hydrocarbon mixtures, which has been compiled from the literature and updated in the present work, and the main reaction pathways through which reactions proceed have been determined and discussed.

METHODOLOGY

Conversion of reactants and formed products during the combustion of a NH_3/CH_4 mixture are studied at high pressures (10, 20, 30, and 40 bar) under well-controlled laboratory-scale conditions. The experimental setup, which has been used in success in previous studies[3,51−53] is schematized in Figure 1. In the present work, a temperature range of 550−1250 K and an oxygen excess ratio (λ) ranging from 0.7−3 have been considered.

The reactant gases are fed from gas cylinders (providers: Air Liquide, Praxair, or Messer) and premixed before entering the quartz flow reactor (153.8 cm long, inner diameter of 0.6 cm), which is placed inside a three-zone electrically heated oven, allowing an isothermal zone inside the tube of approximately 35 cm. This isothermal zone was determined experimentally through the temperature profiles performed at different temperatures and pressures. Figure 2 shows, as an example,

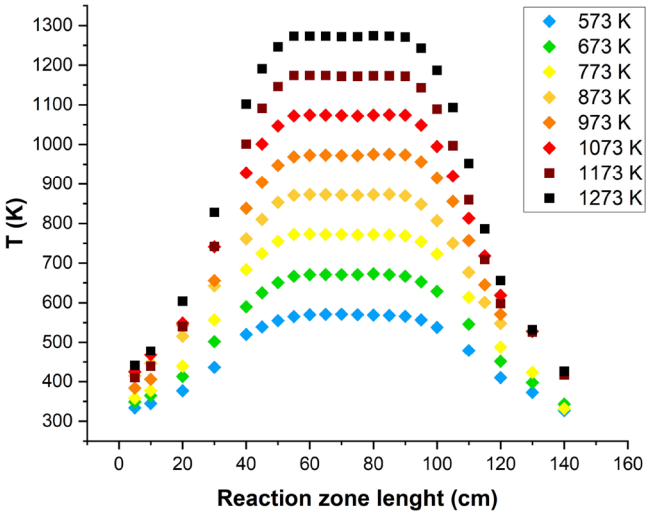

Figure 2. Temperature profiles at 40 bar.

the temperature profiles measured for the pressure of 40 bar, using a gas flow rate of 1000 mL (STP)/min, as has been used in all the experiments. Profiles for the different pressures and temperatures were also determined. The temperature profiles along the reactor were determined using a thermocouple positioned in the space between the quartz tube and the steel shell used to keep the pressure constant. The temperature measurement was taken each 5 cm in the central zone and each 10 cm at both sides of the reactor.

In the present work, the effect of the main variables has been analyzed: oxygen excess ratio (reducing, $\lambda = 0.7$, stoichiometric, $\lambda = 1$, and oxidizing, $\lambda = 3$, conditions), pressure (10, 20, 30, and 40 bar) and temperature (from 550 to 1250 K) and CH_4/NH_3 ratio (0.5, 1, and 2), which means with methane nominal concentration of 500, 1000, and 2000 ppm, respectively, for a nominal ammonia concentration of 1000 ppm.

The oxygen excess ratio (λ) is defined on the basis of the NH_3 oxidation reaction to N_2 (R1) ($4NH_3 + 3O_2 \rightleftharpoons 2N_2 + 6H_2O$) according to eq 1:

$$\lambda = \frac{[O_2]_{inlet}}{[O_2]_{stoichiometric}} \quad (1)$$

The flow rate is 1000 mL (STP)/min and implies a temperature- and pressure-dependent gas residence time in the isothermal reaction zone, as described in eq 2.

$$t_r(s) = 231.6 \times \frac{P(bar)}{T(K)} \quad (2)$$

In the experiments, concentrations of NH_3, CH_4, O_2, H_2, NO, NO_2, N_2O, N_2, CO, CO_2, and HCN are analyzed and quantified with a gas microchromatograph (Agilent Technologies), a $NH_3/NO/NO_2/N_2O$ continuous analyzer (ABB, model: Advance Optima AO2020), a CO/CO_2 continuous analyzer (ABB, model: Advance Optima AO2000) and a Fourier-transform infrared (FTIR) spectroscopy analyzer (Protea, model: ProtIR 204M).

The estimated uncertainty of the measurements is within ±5% but not less than 5 ppm for the continuous analyzers and 10 ppm for the gas microchromatograph and FTIR determinations. As mentioned, mixtures are diluted in argon.

Table 1 summarizes the experimental initial conditions. Sets 17, 22 and 17R, 22R correspond to repetition experiments. The

Table 1. Matrix of Experimental Conditions[a]

set	NH_3 (ppm)	CH_4 (ppm)	O_2 (ppm)	P (bar)	λ
1	1113	560	1246	40	0.64
2	971	504	1772	20	1.02
3	936	545	1709	40	0.95
4	961	527	5234	20	2.95
5	959	507	5198	30	3.00
6	959	550	5313	40	2.92
7	1095	1094	1924	40	0.64
8	925	1085	2915	10	1.02
9	933	1136	2807	20	0.94
10	1092	1100	2646	30	0.88
11	933	1094	2705	40	0.94
12	968	1082	8385	10	2.90
13	915	1073	8456	20	2.99
14	931	1072	8185	30	2.88
15	935	1115	8255	40	2.82
16	1119	2070	3350	40	0.67
17	953	2178	4826	10	0.95
17R	938	2151	4782	10	0.96
18	937	2138	4921	20	0.99
19	983	2137	4850	40	0.97
20	928	2161	14150	20	2.82
21	1093	2055	14049	30	2.85
22	918	2097	13997	40	2.87
22R	1063	2065	14336	40	2.91

[a]All experiments are performed in the 550−1250 K temperature interval with a total flow rate of 1000 mL (STP)/min and using Ar as a bath gas. The residence time is defined by eq 2.

experimental results of repeated experiments will be later compared to evaluate the repetitiveness of the experimental results. The influence of pressure at different temperatures has been evaluated in the 10 to 40 bar range for stoichiometries of 1 and 3 (sets 2−6, 8−15, and 17−22 in Table 1). For the highest pressure studied, 40 bar, we have also considered a fuel-rich stoichiometry of 0.7 (sets 1, 7, and 16 in Table 1), as the

https://doi.org/10.1021/acs.energyfuels.3c03959
Energy Fuels 2024, 38, 1399−1415

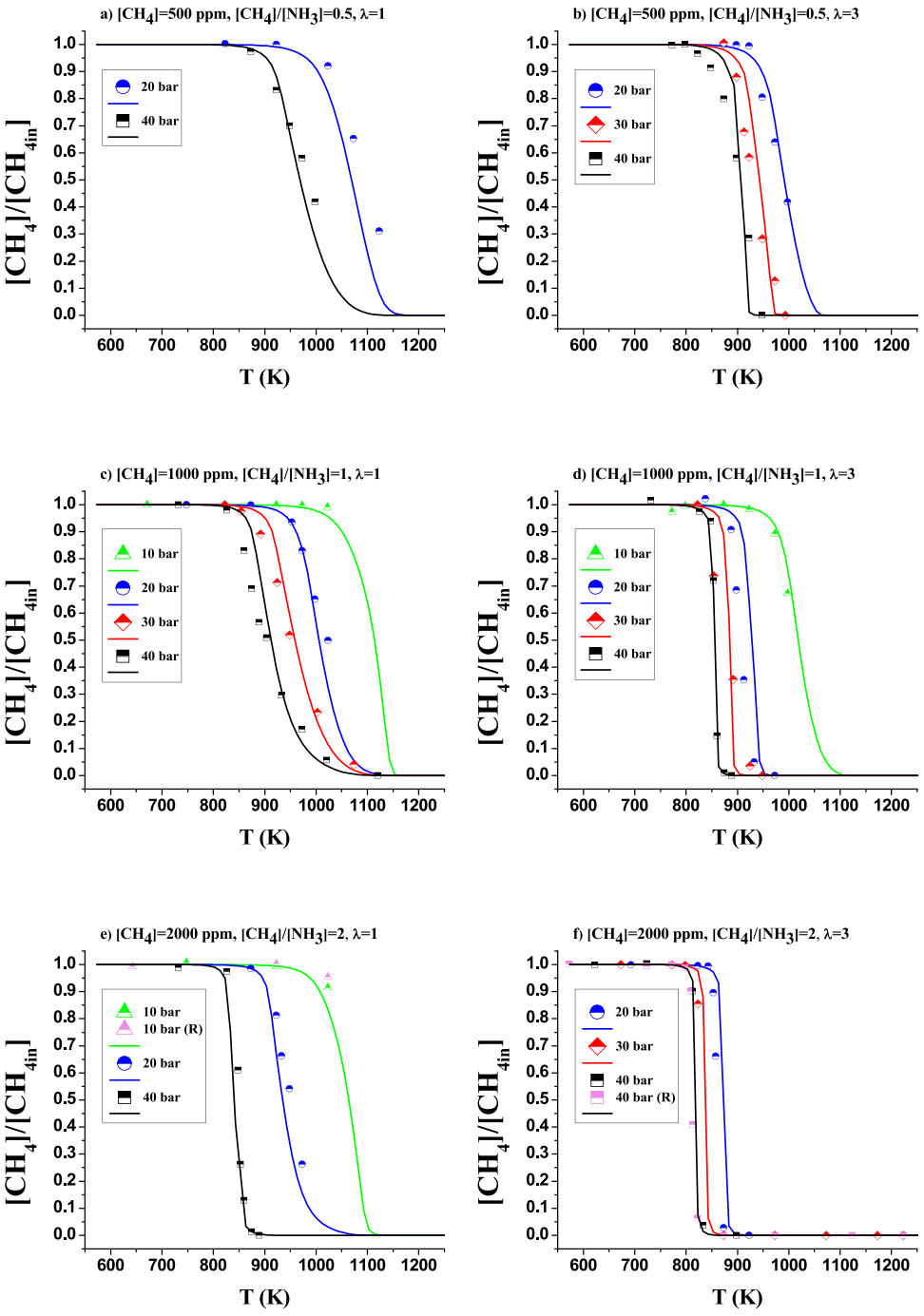

Figure 3. CH_4 conversion as a function of temperature for different pressures (10−40 bar). Sets 2−6, 8−15, and 17−22 in Table 1. [CH_4] = 500 ppm (a, b), 1000 ppm (c, d), and 2000 ppm (e, f). [NH_3] = 1000 ppm. Left column λ = 1 and right column λ = 3. Ar as a bath gas. Symbols are used to represent experimental data and lines for calculations. Residence time is defined by eq 2.

experimental higher pressure conditions allowed us to see the NH_3 reaction at comparatively lower temperatures.

KINETIC MODELING

The experimental results of the present work are simulated using a gas-phase chemical kinetic mechanism based on earlier work on nitrogen chemistry by Glarborg et al.,[54] drawing on more recent work on amine chemistry by Stagni et al.,[55] updated adding an acetonitrile reaction subset by Alzueta et al.[56] as well as a reaction subset of methylamine by Glarborg et al.,[57] updated by Marrodán et al.,[58] and including modifications and/or recommendations of the recent studies of Burke,[59] Klippenstein et al.,[60] Marshall et al.,[61] Alzueta et al.,[13,44] and Glarborg et al.[62−64] Reactions recently revised such as NH_2 + HO_2 by Klippenstein et al.[65] and NH_2 + NO_2 by Glarborg,[64] as well as steps involved in amine pyrolysis[61,63] and H_2NO reactions proposed by Stagni et al.[66] were included as well. Other steps involved in amine chemistry are updated from the work of Cobos and Gao.[67,68]

The mechanism has been extended to include DME conversion including several reaction subsets taken from previous work of Marrodán et al.,[69] which were tested and

https://doi.org/10.1021/acs.energyfuels.3c03959
Energy Fuels 2024, 38, 1399−1415

validated under atmospheric-pressure conditions[70] and modified to consider high-pressure conditions by Marrodán et at.[69,71,72] These modifications include C_1-C_2 and NO interactions, proposed by Glarborg et al.[73] and have been revised and updated according to more recent studies involving NO_x that work developed and validated under high-pressure conditions,[74−78] as well as reaction subsets for compounds such as ethanol, C_2H_2 proposed by Alzueta et al.[79] for atmospheric conditions and modified by Giménez et al.[78] to consider high-pressure conditions. The DME subset taken from the work of Alzueta et al.[80] at atmospheric pressure has been updated according to more recent mechanisms[81,82] to take into account the high-pressure effects. Additionally, the mechanism includes a subset for oxidation of formic acid based on the work of Marshal and Glarborg,[83] reaction subsets for methyl formate,[71] dimethoxymethane,[51] and ethanol[72] taken from different sources, as reported. The thermodynamic data come from the same sources as for the kinetic mechanisms used. The full mechanism is available as the Supporting Information.

The full compiled mechanism with the modifications mentioned has been tested, compared, and validated against several experimental data sets using different experimental setups in a wide range of conditions by Marrodán et al.[69] for DME mixtures.

Calculations have been carried out in the present work using the plug-flow reactor (PFR) model of the Chemkin Pro suite (2016),[84] the initial conditions for each experiment as listed in Table 1, and a "fix gas temperature" type problem, using the nominal reaction temperature at the flat temperature zone since similar results were obtained with and without the measured temperature profiles. The validity of the model and the mechanism has been assessed using different literature studies in which flow reactor data at atmospheric pressure were presented.[12,18] Comparison of literature experimental results, shown in Table S1 of the Supporting Information, and calculations with the mechanism compiled and updated in this work are included in Figures S1 and S2 of the Supporting Information. The performance of the model is very good as well for the atmospheric flow reactor experimental data of Figures S1 and S2, which indicates that the model does a good job simulating the conversion of ammonia/methane mixtures, as will also be seen as follows.

RESULTS AND DISCUSSION

Effect of Pressure. Figure 3 shows the conversion of CH_4 as a function of temperature for different pressures (from 10 to 40 bar), different CH_4/NH_3 ratios (0.5, 1, and 2), and oxygen excess ratios (λ = 1 and 3). Symbols denote experimental results and lines model calculations, from now on. As can be seen, the reaction onset temperature of CH_4 oxidation shows a pressure dependence as also pointed out by other authors.[43] Generally, this temperature decreases markedly with increasing temperature at all pressures studied, as also observed with pure ammonia oxidation at high pressure.[53,85]

For a pressure increase of 20 bar (from 20 to 40 bar), keeping the rest of the conditions similar, the CH_4 oxidation reaction onset temperature decreases under stoichiometric conditions (λ = 1) is 150 K (1025 K → 875 K), 100 K (925 K → 825 K) and 50 K (875 K → 825 K) and under oxidizing conditions (λ = 3) is 75 K (900 K → 825 K), 25 K (850 K → 825 K) and 25 K (825 K → 800 K), for the CH_4/NH_3 ratio of 0.5, 1, and 2, respectively. The different reaction onset temperatures for both NH_3 and CH_4 are summarized in Table S2 of the Supporting Information. Under the current studied conditions, it is noteworthy that, for the same stoichiometry, the higher the CH_4/NH_3 ratio, the lower the effect of pressure on the onset temperature of the CH_4 oxidation reaction. This effect is also observed when we switch from stoichiometric to oxidizing conditions, keeping a similar CH_4/NH_3 ratio. This is in line with the findings of other authors.[12,43]

The experimental results are compared to modeling predictions using the kinetic mechanism previously described. The model generally reproduces very well the trends of CH_4 consumption, for the different pressures under the stoichiometric and oxidizing conditions of Figure 3. Modeling calculations indicate that the full conversion of CH_4 is obtained approximately at the same temperature as those in the experimental results.

CH_4 consumption takes place mainly through H atom abstraction by OH (R8) and by reaction with the amine radical (R9). At the highest temperatures considered, (R8) becomes the main CH_4 consumption reaction under the studied conditions. Alzueta et al.[12] also found (R8) and (R9) as the main CH_4 conversion reaction in a flow reactor study of NH_3/CH_4 oxidation at atmospheric pressure. Under certain conditions, CH_4/NH_3 = 0.5, reaction (R9) is the main CH_4 consumption reaction. This is in line with the findings of Dai et al.[43] who suggest that (R9) becomes more important at CH_4/NH_3 = 0.05 than for CH_4/NH_3 = 0.5.

$$CH_4 + NH_2 \rightleftharpoons CH_3 + NH_3 \quad \text{(R9)}$$

Figure 3 also shows the repeatability of sets 17, 22 and 17R, 22R, respectively. As seen, the reproducibility of the experiments is very good in all the temperature ranges considered, which is an indication of the good performance of the experimental system and experimental procedure.

To get some insight into the reaction pathway through which the oxidation conversion of CH_4 in the presence of NH_3 proceeds at high pressure and different stoichiometries, we have made reaction pathway analyses for the different conditions considered. Figure 4 shows the reaction path diagram for CH_4 consumption at $[CH_4]$ = 1000 ppm, and λ = 1 and 3 for the highest (40 bar) and lowest (10 bar) studied pressures when 10% of the NH_3 is consumed. The only difference observed occurs at λ = 1 and 10 bar (green). In any case, at the end, the

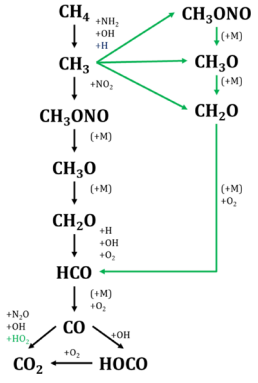

Figure 4. Reaction path diagram for consumption of CH_4 at CH_4/NH_3 = 1 for reducing (λ = 0.7) at 40 bar, stoichiometric (λ = 1) and oxidizing (λ = 3) conditions at 10 and 40 bar. Sets 7, 8, 11, 12, and 15 on Table 1. Black lines represent the common path for the different conditions, and green lines show the additional path happening at 10 bar.

https://doi.org/10.1021/acs.energyfuels.3c03959
Energy Fuels 2024, 38, 1399−1415

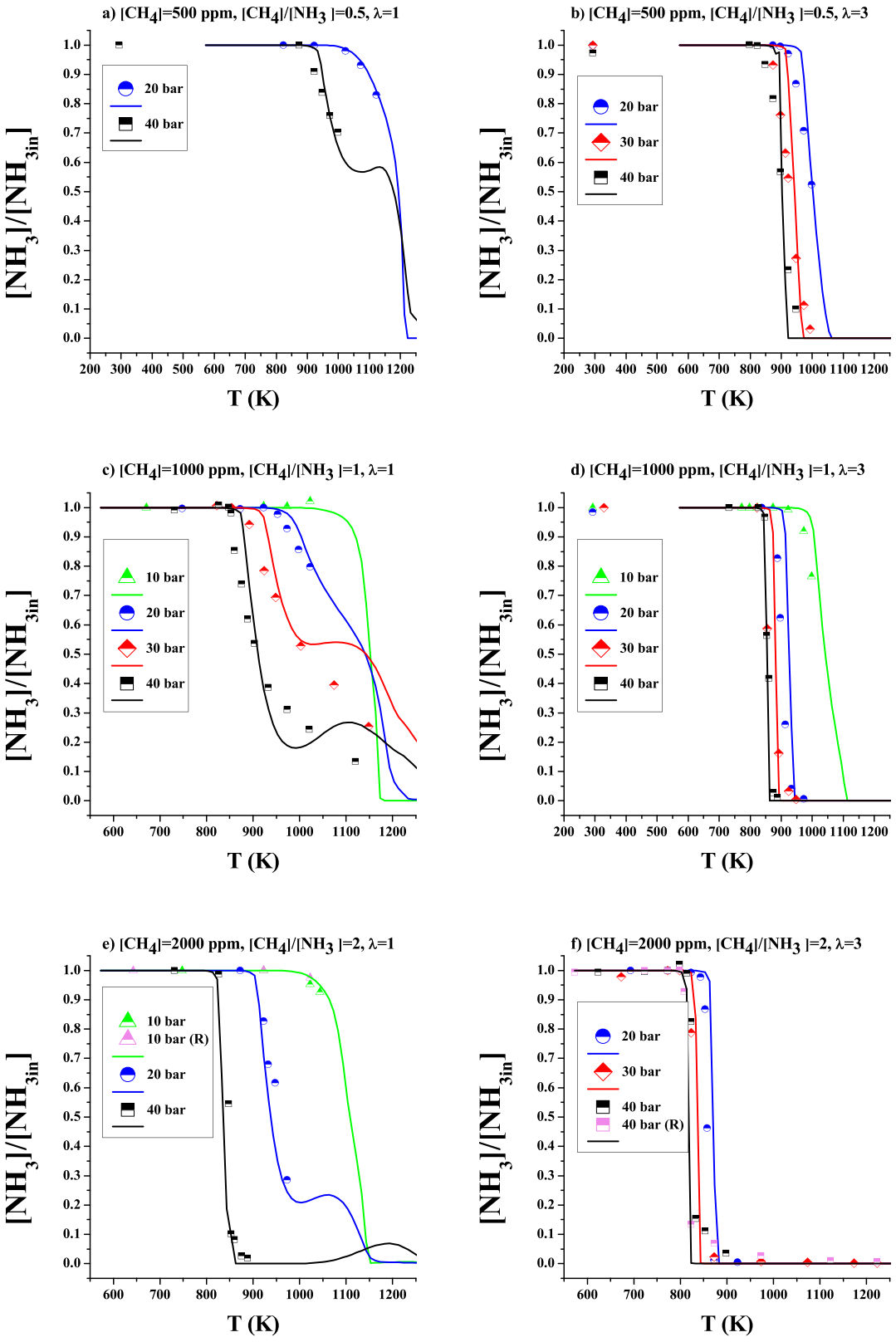

Figure 5. NH_3 conversion as a function of temperature for different pressures (10−40 bar). Sets 2−6, 8−15, and 17−22 in Table 1. $[CH_4]$ = 500 ppm (a, b), 1000 ppm (c, d), and 2000 ppm (e, f), $[NH_3]$ = 1000 ppm. Left column λ = 1 and right column λ = 3. Ar as a bath gas. Symbols are used to represent experimental data and lines for calculations. Residence time is defined by eq 2.

same species are involved, producing CO and CO_2 as a general reactor output product.

The species and pathways marked in green are important only for 10 bar and stoichiometric conditions. As can be seen, the sequence $CH_4 \rightarrow CH_3 \rightarrow CH_3ONO \rightarrow CH_3O \rightarrow CH_2O \rightarrow HCO \rightarrow CO \rightarrow CO_2$ is the major CH_4 consumption channel.

Figure 5 shows the conversion of NH_3 as a function of temperature for different pressures (from 10 to 40 bar), different

https://doi.org/10.1021/acs.energyfuels.3c03959
Energy Fuels 2024, 38, 1399−1415

CH_4/NH_3 ratios (0.5, 1 and 2) and oxygen excess ratios (λ = 1 and 3), i.e., similar conditions as Figure 3. For any pressure studied, the NH_3 consumption shows the same reaction tendency as CH_4 as the temperature increases. The NH_3 concentration is sharply reduced at a given temperature. Both the NH_3 oxidation onset temperature and the decrease of the onset temperature for NH_3 consumption due to the pressure increase coincide with those given above for CH_4. This effect also happens at atmospheric pressure where both species began to be consumed at the same temperature.[12] As can be seen in Figure 5, the pressure effect on the onset reaction temperature is more pronounced under stoichiometric conditions than at oxidizing ones, contrary to what happens for pure ammonia oxidation,[53] where the pressure increase had an effect independent of the stoichiometry. Thus, bearing in mind the use of ammonia as a fuel, its mixtures with methane provide us benefits when working with excess oxygen and increasing the pressure due to the decrease in the NH_3 oxidation reaction onset temperature from 1100 K[53] to 800 K for CH_4/NH_3 = 0 and 2, respectively, at 40 bar.

For a given stoichiometry, the pressure effect is more pronounced at lower CH_4/NH_3 ratios. The conditions under which an increase in pressure is least noticeable are CH_4/NH_3 = 2 and λ = 3 (Figure 5). In all studied cases of NH_3 oxidation, NH_3 starts to be consumed by reaction (R2) as well known in the literature.[12,13,53]

Figure 5 e,f, shows the repeatability of sets 17, 22 and 17R, 22R conditions, respectively. As for CH_4, the reproducibility of the experiments is very good in all the temperature range considered.

Figure 6 shows the NH_3 consumption reaction path for CH_4/NH_3 = 1. On the left, for λ = 0.7 at 40 bar and λ = 1 at 10 (green)

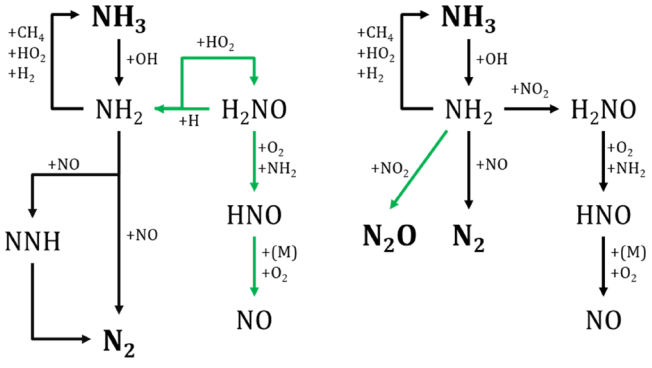

Figure 6. Reaction path diagram for the consumption of NH_3 at CH_4/NH_3 = 1 for reducing conditions (λ = 0.7) at 40 bar and stoichiometric conditions (λ = 1) at 10 and 40 bar (left) and, oxidizing conditions (λ = 3) at 10 and 40 bar (right). Black lines represent the common path for the different conditions and green lines show the additional path happening at 10 bar (left) and 40 bar (right).

and 40 bar. On the right, for λ = 3 at 10 and 40 bar (green). In both cases, black lines represent the common path for the different conditions studied. As can be seen in Figure 6, $NH_3 \rightarrow NH_2 \rightarrow H_2NO \rightarrow HNO \rightarrow NO$ and $NH_3 \rightarrow NH_2 \rightarrow N_2$ are the major consumption NH_3 reaction channels: NO reacts with HO_2 to form NO_2, and with NH_2 to form N_2. The produced NO_2 is quickly consumed by reaction with CH_3 to form CH_3ONO and with NH_2 to form H_2NO; thus, no appreciable quantities of this species are found at the reactor outlet.

We also performed sensitivity analysis. Figure 7 shows an example of the results obtained for CH_4/NH_3 = 1, at 40 bar and λ = 1 at 878 K. CH_4 consumption is promoted by its reaction with NH_2, OH, and HO_2 to form CH_3 radicals, by the reaction of CH_2O with HO_2, OH, and O_2 to form HCO, by reaction of HO_2 radical with nitrogen species (NH_3, NH_2, NO) to form OH radicals[43] and by reaction of CH_3 radicals with O_2 also to form OH radicals. Under the same experimental conditions, the reaction of NH_3 with OH to form NH_2 and H_2O, and the resulting chain reaction of NH_2 with NO to form N_2 and H_2O and with HO_2 to form NH_3 and O_2, together with the HO_2 recombination to form H_2O_2 and O_2,[43] represent the major inhibition reactions for the consumption of CH_4. In a minor extent, $CH_4 + O_2 \rightleftharpoons CH_3 + HO_2$ (R10) and $2CH_3$ (+M) $\rightleftharpoons C_2H_6$ (+M) (R11) appear as inhibition reactions as well. In the case of NH_3, under the same experimental conditions, its conversion is promoted by the reaction of CH_4 with radicals (NH_2, OH, and HO_2) to form CH_3 radicals, by reactions of HO_2 with other species (NH_2, NO and NH_3) to form OH radicals, by reaction of CH_3 radicals with O_2 to form also OH radicals, by reactions of CH_2O with oxygenated species (OH, HO_2 and O_2) to produce HCO and by reaction of NH_2 radicals with NO_2 to form NO. As can be seen in the CH_4 case, the consumption of NH_3 is promoted by the production of OH, CH_3, and HCO species. In this case, for the inhibition of NH_3 consumption, we find reaction (R10) $CH_4 + O_2 \rightleftharpoons CH_3 + HO_2$ and the recombination reactions (R11) $2CH_3$ (+M) $\rightleftharpoons C_2H_6$ (+M) and (R12) $2HO_2 \rightleftharpoons H_2O_2$ and the NH_3 chain reaction of (R2) $NH_3 + OH \rightleftharpoons NH_2 + H_2O$, followed by (R3) $NH_2 + NO \rightleftharpoons N_2 + H_2O$ or (R13) $NH_2 + HO_2 \rightleftharpoons NH_3 + O_2$. As with CH_4, the inhibition of ammonia combustion is favored by reactions that produce HO_2, H_2O, and O_2 species. It can be considered that as the main trends of species conversion are well captured by the model, the main reaction pathways are feasible.

The main products measured in significant amounts during the conversion of NH_3/CH_4 mixtures are NO, N_2O, N_2, H_2, CO, and CO_2. N_2 and N_2O are the most abundant nitrogen species since NO is consumed by reaction with NH_3.[44] NO_2 is below 10 ppm in all studied experimental conditions, which is consistent with the results of the previous studies for pure ammonia oxidation.[53] Figures S3 and S4 of the Supporting Information compare, respectively, experimental and simulated results of N_2 and NO obtained during the oxidation of NH_3 in its mixtures with CH_4 at different oxygen excess ratios for each pressure studied. NO is produced under oxidizing conditions and CH_4/NH_3 = 1 and 2. Model calculations reproduce well the experimental observations. NO production does not follow a clear trend with varying pressure, with NO concentration increasing with pressure for CH_4/NH_3 = 1 and decreasing for CH_4/NH_3 = 2 with a similar pressure variation (Figure S4). Also, the difference in the concentration of NO produced is not remarkable. For the same pressure, NO production is favored by CH_4 addition, with a peak of 16 ppm for CH_4/NH_3 = 1 and 36 ppm for CH_4/NH_3 = 2. Probably, the diminution of the NH_3 ratio in the mixture provokes this NO increase in the exhaust gases,[28] which is a drawback of using mixtures with high CH_4/NH_3 ratios. The main production reaction of NO is (R14) and to a minor extent (R15), (R16) and (R17). It is noted that (R15) and (R16) are more noticeable for λ = 3 than λ = 1, and (R17) is only remarkable at the highest pressures.

$$CH_3O + NO(+M) \rightleftharpoons CH_3ONO(+M) \quad \text{(R14)}$$

https://doi.org/10.1021/acs.energyfuels.3c03959
Energy Fuels 2024, 38, 1399−1415

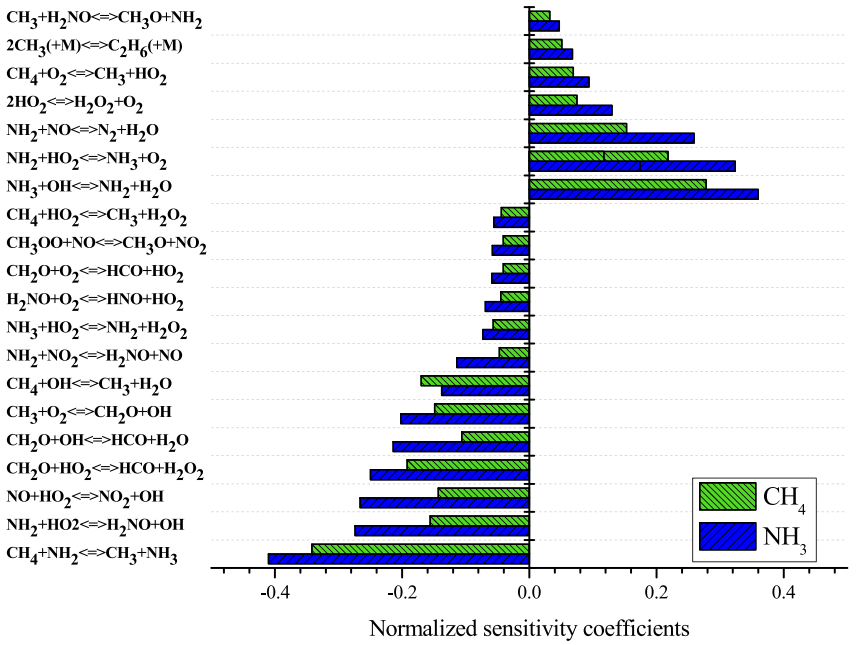

Figure 7. Sensitivity analysis for NH_3 and CH_4 conversion under the experimental conditions of Set 11 in Table 1, $CH_4/NH_3 = 1$, 40 bar, $\lambda = 1$ at 878 K.

$$HNO + O_2 \rightleftharpoons HO_2 + NO \quad (R15)$$

$$NH_2 + NO_2 \rightleftharpoons H_2NO + NO \quad (R16)$$

$$NO + OH(+M) \rightleftharpoons HONO(+M) \quad (R17)$$

NO is consumed mainly through reaction (R18) to form NO_2 and to a minor extent via reactions (R3) and (R4) to form N_2 and NNH.

$$NO + HO_2 \rightleftharpoons NO_2 + OH \quad (R18)$$

This is consistent with the results obtained in our previous work on high-pressure ammonia consumption in a flow reactor[53] in which NO was not produced under stoichiometric conditions. The typical thermal DeNO$_x$ reaction $NH_2 + NO \rightleftharpoons NNH + OH$ has not been found to be very important under the studied conditions, as other authors have.[20]

In contrast, we found a clear effect of pressure on the N_2O concentration at the reactor output, which consists of obtaining a higher N_2O concentration at higher working pressures. A direct relationship has also been found between the CH_4/NH_3 ratio and the N_2O production, which will be discussed below. Figure 8 (rescaled as Figure S5 in the Supporting Information) shows the results of N_2O concentration as a function of temperature. In that figure, a maximum of 140, 215, and 290 ppm of N_2O at 40 bar at $\lambda = 3$ for CH_4/NH_3 ratios of 0.5, 1, and 2, respectively is observed. Model calculations reproduce the main trends observed experimentally, even though they underpredict the specific values. The model simulations indicated that the N_2O concentration is very low under all studied conditions, but, as can be seen in Figure 8, this does not occur experimentally, where concentrations are higher than calculations. According to the model, the production of N_2O takes place through reactions (R19) and (R20), in comparison to atmospheric pressure where this occurs exclusively via (R20).[18]

$$NH_2 + NO_2 \rightleftharpoons N_2O + H_2O \quad (R19)$$

$$NH + NO \rightleftharpoons N_2O + H \quad (R20)$$

In the presence of CH_4 with high concentration levels of CO, N_2O consumption mainly occurs through reaction (R21) as found by Sun et al.[20] and to a minor extent through reaction.

$$CO + N_2O \rightleftharpoons N_2 + CO_2 \quad (R21)$$

$$N_2O(+M) \rightleftharpoons N_2 + O(+M) \quad (R22)$$

Concerning N_2, this species is produced by reaction (R3) and to a minor extent by reaction (R5). It is noticeable that at intermediates and high temperatures, in which the NH_3 concentration is below 50%, (R21) starts to be important in N_2 production.

Regarding CO, in Figure 9, CO is produced through reactions (R23) and (R24) under all studied conditions. Reaction (R24) is favored by the increase in pressure, which is even more noticeable under oxidizing conditions. Also, as the CH_4/NH_3 ratio increases, this effect is accentuated, with the (R23) reaction being negligible at $CH_4/NH_3 = 2$.

$$HCO(+M) \rightleftharpoons H + CO(+M) \quad (R23)$$

$$HCO + O_2 \rightleftharpoons CO + HO_2 \quad (R24)$$

CO is then consumed to produce CO_2 by (R21), (R25) and (R26) reactions and to produce HOCO, via reaction (R21), which is then converted to CO_2 by oxidation (R28).

$$CO + OH \rightleftharpoons CO_2 + H \quad (R25)$$

$$CO + HO_2 \rightleftharpoons CO_2 + H_2 \quad (R26)$$

$$CO + OH \rightleftharpoons HOCO \quad (R27)$$

$$HOCO + O_2 \rightleftharpoons CO_2 + HO_2 \quad (R28)$$

As far as consumption reactions are concerned, while (R25) is always present, (R26) is important only for the lowest pressure studied and (R27) and (R28) for the higher pressure conditions considered.

We have evidenced some instability in calculations with the model under the given conditions. This issue is more relevant as the pressure increases, in particular, for stoichiometric

https://doi.org/10.1021/acs.energyfuels.3c03959
Energy Fuels 2024, 38, 1399−1415

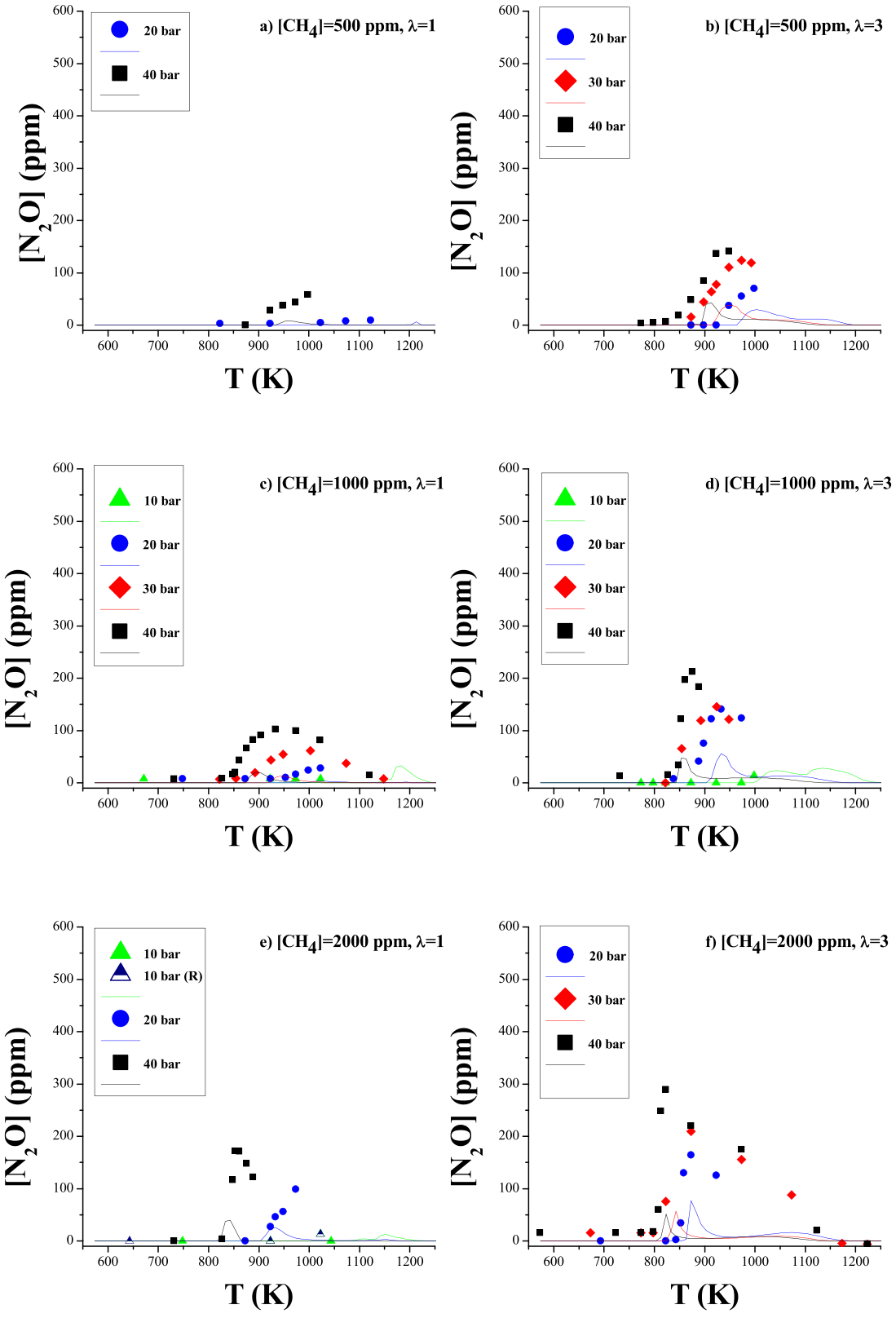

Figure 8. N_2O production as a function of temperature for different pressures (10−40 bar). Sets 2−6, 8−15 and 17−22 in Table 1. $[CH_4]$ = 500 ppm (a, b), 1000 ppm (c, d), and 2000 ppm (e, f). $[NH_3]$ = 1000 ppm. Left column λ = 1 and right column λ = 3. Ar as a bath gas. Symbols are used to represent experimental data, and lines for calculations. Residence time is defined by eq 2.

conditions. In order to analyze this in certain detail, we performed some tests. It is found that the reaction $NH_2 + HO_2 \rightarrow$ products is a key step as pointed out[43,85] and the possible product channels of this reaction are (R13), (R29), and (R30). Therefore, optimizing the mechanism of NH_3 conversion for high pressure needs to take into account the rate constant of H_2NO-related reactions, which have been reported to be relevant.[85] At present, we do not know the reason for the

https://doi.org/10.1021/acs.energyfuels.3c03959
Energy Fuels 2024, 38, 1399−1415

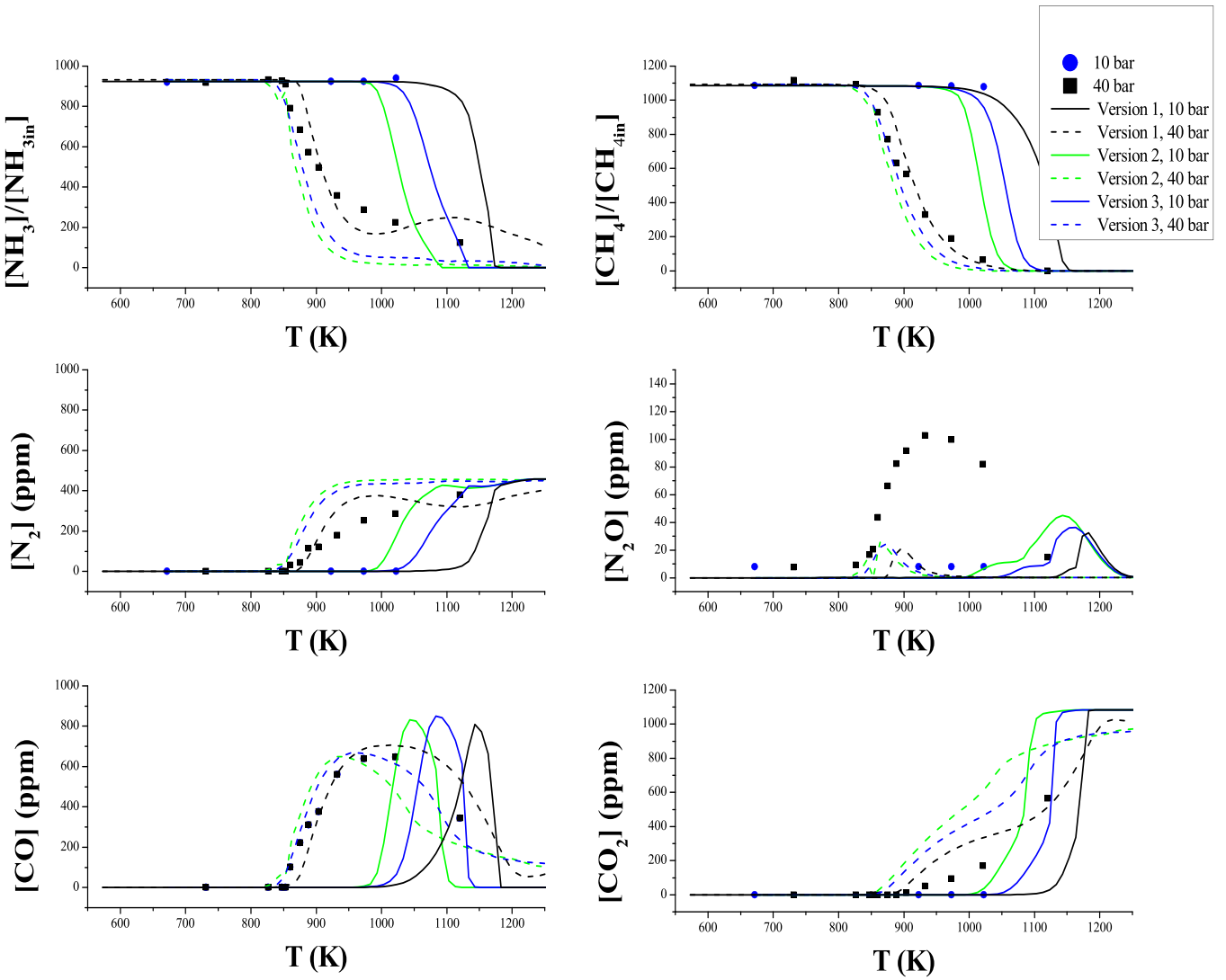

Figure 9. Experimental (symbols) and simulated (lines) results as a function of temperature for different pressures (10−40 bar) and $\lambda = 1$. Sets 8−11 in Table 1. $[CH_4]$ = 1000 ppm $[NH_3]$ = 1000 ppm. Ar as a bath gas. Residence time is defined by eq 2.

discrepancy between the experimental and calculation results, but this is an aspect that deserves further specific studies.

$$NH_2 + HO_2 \rightleftharpoons HNO + H_2O \quad \text{(R29)}$$

$$NH_2 + HO_2 \rightleftharpoons H_2NO + OH \quad \text{(R30)}$$

Figure 9 shows the experimental and simulation results of consumption and production of the species suffering from these instabilities (i.e., NH_3, N_2, and CO) with three different modifications of the current mechanism used. First, the mechanism of the present work using the reaction rates constants proposed by Klippenstein et al.[65] for reactions (R13), (R29), and (R30) without modifications (version 1 of the mechanism). Then, we have used two other versions of the mechanism: one using the rate constants of Sumathi et al.[86] for reactions (R13), (R29), and (R30) (version 2 of the mechanism), and the same mechanism of version 1, in which reaction (R30) has been multiplied by 10 (version 3 of the mechanism). With both versions 2 and 3 of the mechanism, instabilities disappear (Figure 9), and the changes made in version 3 resulted in a large overprediction of N_2 and CO_2. Thus, we can state that the most critical reaction when it comes to produce instabilities is reaction (R30), where the rate value appears to be critical for the model performance.

The instability issue may also be attributed to thermochemical data of participating species, mainly HNO, or to the evolution of the H_2NO species which has been identified as important in other ammonia studies.[54]

As seen in Figure 9, the best match of the experimental results and calculations made with the 3 versions of the mechanism is obtained with version 3. As has been mentioned, multiplying the rate constant of reaction (R30) by 10 acts to avoid the instabilities happening with the mechanism proposed in the present work, i.e., version 1, which includes without changes the rate constant proposed by Klippenstein et al.[65] Version 2 of the mechanism includes the rate constants of Sumathi et al.[86] for reactions (R13), (R29), and (R30), and also avoids instabilities, even though it largely overpredicts the conversion of NH_3 and production of N_2 and CO_2. For the N_2O production cases, none of the 3 versions solve the problem of instabilities. Additionally, it has to be noted that the recent work by Klippenstein and Glarborg on the reaction rate of $NH_2 + HO_2$ is probably more accurate than the factor of 10 used in version 3 of the mechanism, as necessary to minimize instabilities, since that

https://doi.org/10.1021/acs.energyfuels.3c03959
Energy Fuels 2024, 38, 1399−1415

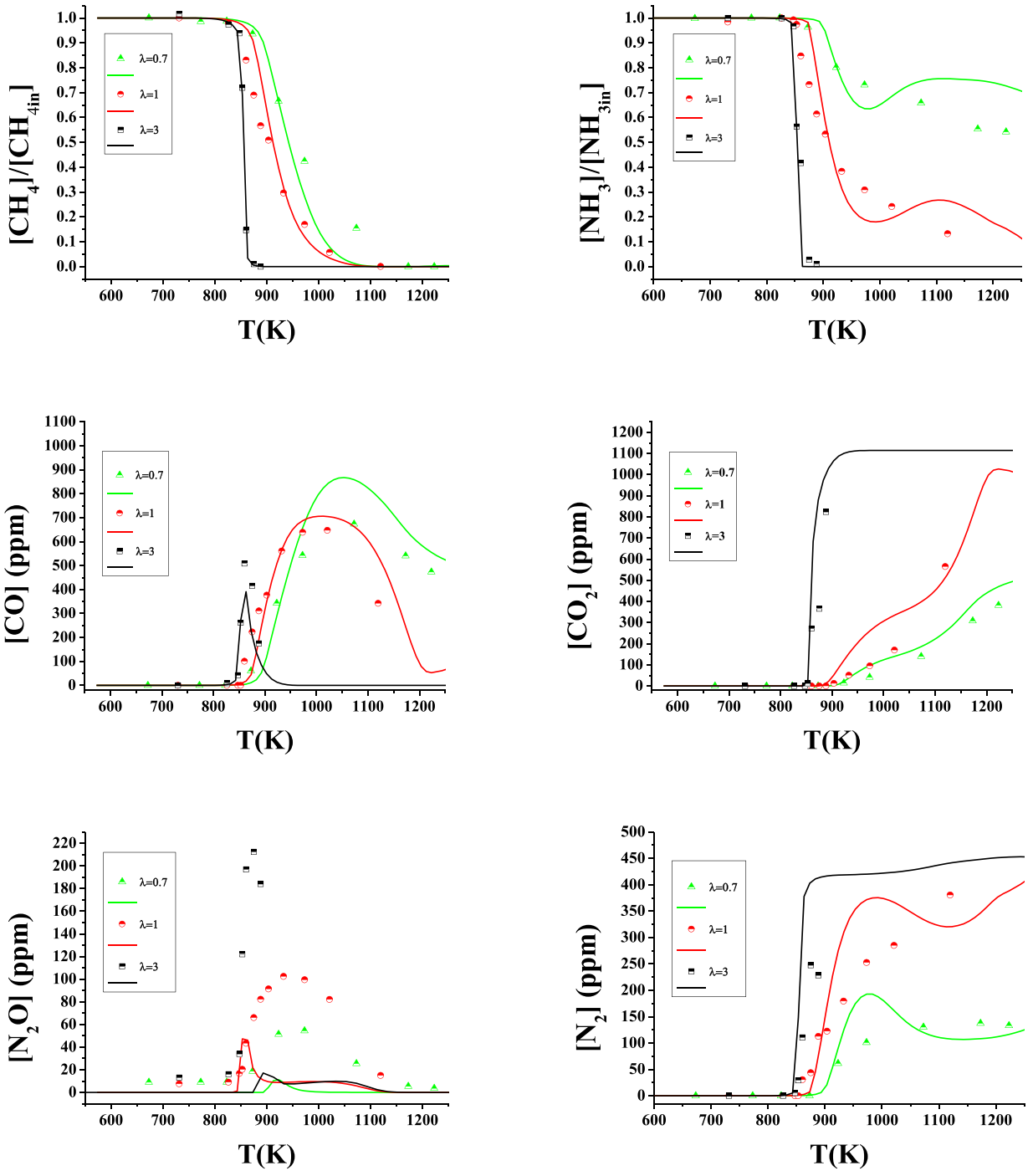

Figure 10. Conversion of NH_3, CH_4, CO, CO_2, N_2O and N_2 as a function of temperature at 40 bar and different stoichiometries. Ar as a bath gas. Sets 7, 11, and 15 in Table 1. (λ = 0.64:1095 ppm of NH_3, 1094 ppm of CH_4; λ = 0.94:933 ppm of NH_3, 1094 ppm of CH_4; λ = 2.82:935 ppm of NH_3, 1115 ppm of CH_4).

determination would exhibit an uncertainty lower than an order of magnitude. However, the use of the 3 modified versions of the mechanism does intend to show that the model still needs improvement, and more work on this is desirable. A possible way for improvement may rely on the formation of C/N species, such as methylamine or a higher amount of nitromethane, whose description may also need refinement. A hypothetical formation of PAH may also happen, in particular under fuel-rich conditions.

As discussed in previous work by our group,[3,51,53,58,69,71,72,87] it is important to bear in mind that the changing in pressure in our experimental system and procedure, implies the change of the residence time according to eq 2, as has been discussed and analyzed in earlier studies.[53,69,87] In these studies, it was concluded that both pressure and residence time simultaneously affected the formation and concentration of products. Compared to the work of Marrodán et al.,[69,87] in the present results, pressure has a major influence on the methane and ammonia conversion, as can be seen in Figures S6 and S7 of the Supporting Information.

Effect of the Oxygen Excess Ratio. Figure 10 includes the results of varying the oxygen excess ratio (λ = 0.7, 1 and 3) at 40

https://doi.org/10.1021/acs.energyfuels.3c03959
Energy Fuels 2024, 38, 1399−1415

bar for CH_4/NH_3 = 1, to show the effect of the availability of O_2 availability. Experimental results show a clear sensitivity to oxygen availability. Reactant conversion is shifted to lower temperatures when the O_2 concentration is increased. Full conversion, where possible under the conditions studied, is also achieved at lower temperatures and higher oxygen concentrations. As the working pressure decreases, the decrease in reaction onset temperature is more pronounced, and the same effect occurs at lower CH_4/NH_3 ratios. Switching from stoichiometric to oxidizing conditions, at 20 bar, the reaction onset temperature reduction is 125, 75, and 50 K, for CH_4/NH_3 = 0.5, 1, and 2. Changing from λ = 0.7 to 1 produces only a shift (50 K) for CH_4/NH_3 = 0.5 and 1. In the case of 40 bar and at CH_4/NH_3 = 1 (Figure 10), a shift to a lower temperature of the onset of the CH_4 and NH_3 conversion reaction has been found (50 K, 875 → 825) when moving from reducing to oxidizing conditions. In previous work of our group, it was found that the conversion of pure ammonia happens at approximately 20−25 K[53] less under oxidizing conditions compared to stoichiometric conditions. However, when CH_4 is added, this difference increases, as seen in the present results. Methane is mainly consumed by H-abstraction-producing CH_3 radicals, which leads to the increase of the O/H radical pool. Also, the addition of methane leads to the production of CH_3, CH_2O, and HCO, species that promote ammonia consumption, as can be seen in the results of the sensitivity analysis of Figure 7.

The maximum peak of CO emissions is reached at lower temperatures and in lower concentrations with increasing excess oxygen ratio, which logically promotes full CO conversion; therefore, CO_2 production is shifted to lower temperatures. From an environmental point of view, it is remarkable that the increase in pressure leads to an increase in the maximum N_2O concentration observed, as pointed out before, increasing it by a factor of more than 2 when switching from stoichiometric to oxidizing conditions.

One key consideration to bear in mind when discussing a deficiency or excess of oxygen is the production of HCN. In our experimental system, under the studied conditions, it has been found that HCN is only produced under reducing conditions. Under these conditions, the HCN concentration at the outlet is higher as the proportion of CH_4 is higher in the mixture. Figure 11 includes the results of HCN production varying the oxygen excess ratio (λ = 0.7 and 3) at 40 bar for CH_4/NH_3 = 2 (the most favorable CH_4/NH_3 ratio for HCN formation) and varying the CH_4/NH_3 ratio under reducing conditions, to show the effect of both O_2 availability and CH_4/NH_3 ratio. Results show that, for λ = 0.7, an appreciable formation of HCN happens during the interaction between NH_3 and CH_4, in particular, above 1000 K when significant conversion of CH_4 occurs. The model underpredicts the concentration of HCN by a factor of 2, even though the main trends are reasonably well captured. However, no significant formation of HCN is found for fuel-lean conditions, λ= 3.

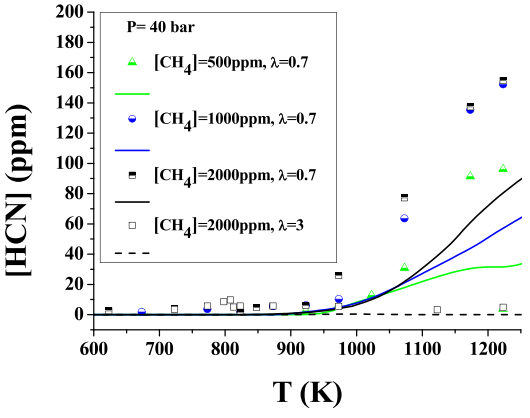

Figure 11. HCN conversion as a function of the temperature at 40 bar and different stoichiometries. Ar as a bath gas. Sets 1, 7, 16, and 22 are shown in Table 1 (λ = 0.64:1113 ppm of NH_3, 560 ppm of CH_4; λ = 0.64:1095 ppm of NH_3, 1094 ppm of CH_4; λ = 0.67:1119 ppm of NH_3, 2070 ppm of CH_4; λ = 2.87:918 ppm of NH_3, 2097 ppm of CH_4).

Effects of the CH_4/NH_3 Ratio. From a practical point of view, it is interesting to evaluate different CH_4/NH_3 ratios in order to assess the use of possible different mixtures containing both ammonia and methane.

The consumption and production of species during the oxidation of CH_4/NH_3 mixtures are also measured as a function of the CH_4/NH_3 ratio, at different oxygen excess ratios (λ = 1 and 3), at 40 bar as an example. To give an idea of the CH_4 addition effect, Figure 12 shows the consumption of CH_4, NH_3, and the production of N_2O. As seen in Figure 12, for a given pressure and oxygen excess ratio, the addition of CH_4 always results in a decrease of the reaction onset temperature of both NH_3 and CH_4 oxidation. This effect is more noticeable for stoichiometric conditions than for oxidizing ones. This fact is of interest, from a practical point of view, because it appears that the addition of carbon combustibles helps to diminish the ignition temperature of ammonia. For the highest pressure studied, 40 bar, pure ammonia starts to convert at approximately 1165 K under the same experimental conditions and [NH_3] = 1000 ppm. In Figure 12, it can be seen that the onset temperature for NH_3 conversion decreases (875 K, 825 K, 825 K, at 40 bar and CH_4/NH_3 = 0.5, 1, and 2, respectively) when NH_3 is oxidized in the presence of CH_4, for all studied CH_4/NH_3 ratios and stoichiometries. This is due to the increased production of OH radicals and CH_3 radicals, which will subsequently produce more OH radicals, as discussed above. On the other hand, the major disadvantage is the production of NO and N_2O occurs at high CH_4/NH_3 ratios. As seen above, the combustion of NH_3 and CH_4 under the studied conditions produces CH_3ONO which decomposes into NO, which reacts to form NO_2 at high pressure, and this later produces N_2O. According to the mechanism, under the present conditions, the increase in N_2O was not found to come from the production of HCN oxidation, as found by other authors,[88,89] even though the specific operating conditions considered are different. Anyway, HCN production is not important under the conditions in which N_2O is formed. In this sense, working with CH_4/NH_3 ratios higher than 1 is not desirable because it does not offer great benefits compared to CH_4/NH_3 ratios of 1 or 0.5, while it leads to a considerable increase of N_2O emitted, which is a greenhouse gas with 273 times more global warming potential than that of CO_2.[90] Furthermore, a high CH_4/NH_3 concentration leads to increased emissions of CO_2.

Mass Balances. In order to evaluate the quality of our experiments and to determine if the measured species are dominant under the studied conditions, we decided to do nitrogen balances for the experiments performed. We can do that because we have used argon as a bath gas, allowing in this way the precise determination of N_2 as a product gas. Figure 13 shows, as an example, a nitrogen atom balance for different experimental conditions. The N balance is calculated by considering the nitrogen atoms of the following species: NH_3,

https://doi.org/10.1021/acs.energyfuels.3c03959
Energy Fuels 2024, 38, 1399−1415

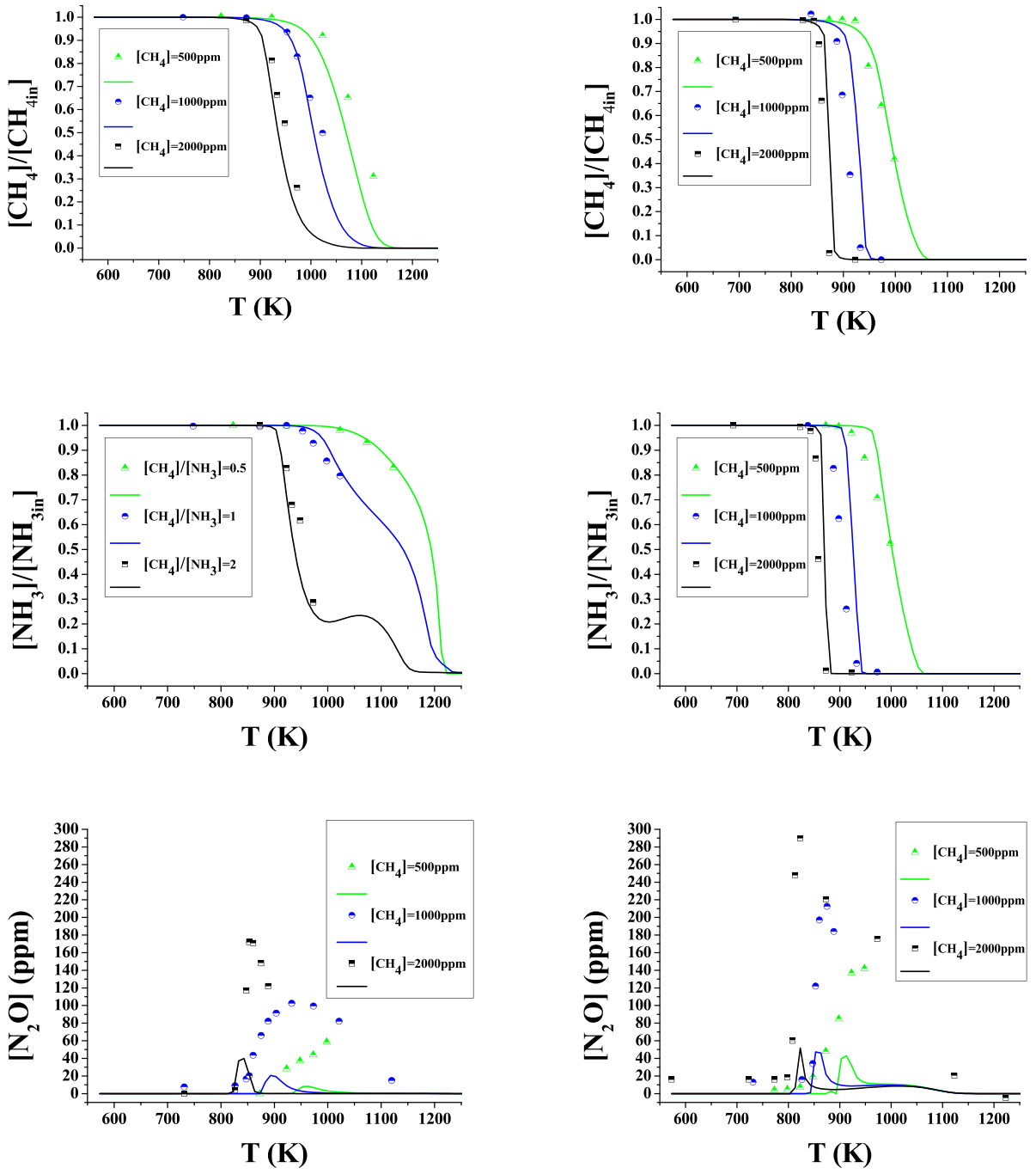

Figure 12. Conversion of NH_3, CH_4, CO, CO_2, N_2O, and N_2 at 40 bar of pressure as a function of temperature and for different CH_4/NH_3 ratios (0.5, 1 and 3). Ar as a bath gas. Sets 3, 6, 11, 15, 19, and 22. Left column $\lambda = 1$ and right column $\lambda = 3$.

N_2, HCN, NO, N_2O, and NO_2. Even though NO_2 has been accounted for in the nitrogen balance determined, their experiment profiles have not been shown in the figures because these species are around the uncertainty of the equipment measurements lower than 5 ppm in all cases. The N balance (in percentage) calculated with the model considering the same species mentioned above is also shown in Figure 13 as a continuous line. As seen, the calculated N balance is between 90 and 100%, while the experimental one closes between 90 and 105% along the whole temperature range. This indicates a reasonable agreement between species determined and calculated, even though a small mass of other species not analyzed experimentally may also be present.

Similarly, Figure 14 shows an example of a carbon atom balance for the same experiments shown in Figure 13. The C balance is calculated considering the carbon atoms of the following species: CH_4, CO, HCN, and CO_2. The C balance (in percentage) calculated with the model of the species mentioned above is also shown in Figure 14 as a line, and it is between 85 and 100%, while the experimental one closes between 90 and 105% for all studied temperatures. Results indicate a reasonable closing of the C balance as well.

CONCLUSIONS

An experimental and simulation study of the main features of the oxidation of mixtures of ammonia with methane at high pressure

https://doi.org/10.1021/acs.energyfuels.3c03959
Energy Fuels 2024, 38, 1399−1415

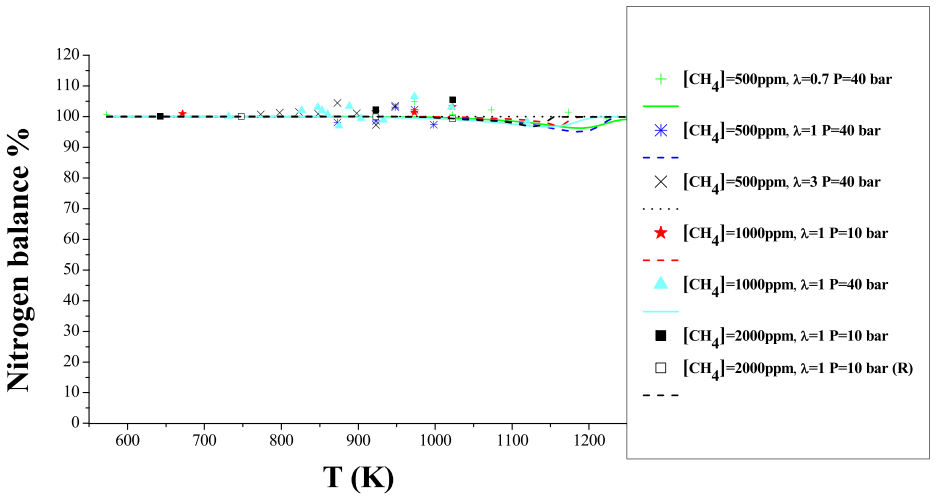

Figure 13. Experimental and calculated N balance during the oxidation of NH_3, as a function of the reactor temperature, for different oxygen excess ratios, compositions, and pressures. Species included in the balance are NH_3, NO, NO_2, N_2O, HCN, and N_2. Sets 1, 3, 6, 8, 11, 22, and 22R are shown in Table 1.

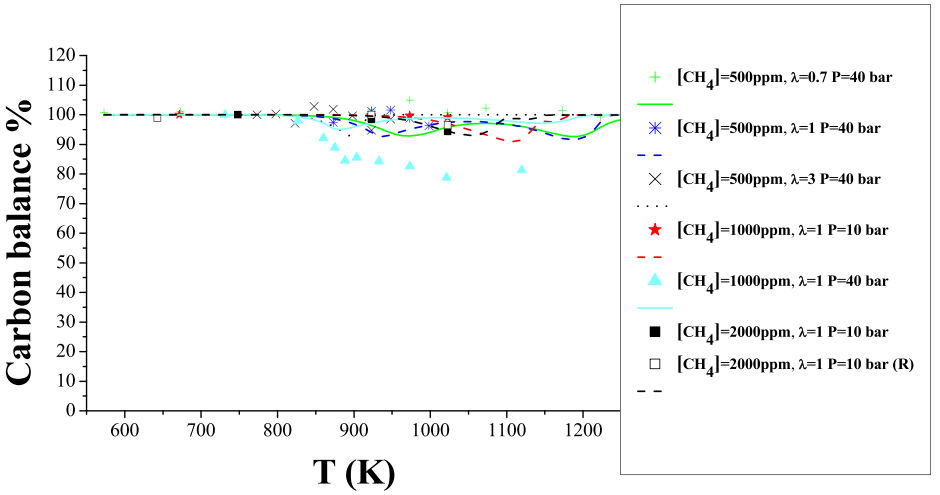

Figure 14. Experimental and calculated C balance during the oxidation of CH_4, as a function of the reactor temperature, for different oxygen excess ratios, compositions, and pressures. Species included in the balance are CH_4, CO, HCN, and CO_2. Sets 1, 3, 6, 8, 11, 22, and 22R in Table 1.

(from 10 to 40 bar), under reducing, stoichiometric, and oxidizing conditions in the 550−1250 K temperature interval, in a quartz tubular flow reactor with, roughly, 1000 ppm of inlet NH_3 and 500, 1000, and 2000 ppm of CH_4, in NH_3/CH_4 mixture, and using argon as a diluent, has been performed.

The main product of ammonia conversion is N_2, followed by N_2O, and under certain conditions NO (CH_4/NH_3 = 1 and 3 at λ = 3) while the NO_2 concentration is negligible and below the uncertainty of the measurements under all conditions studied. The use of high pressure acts to favor the formation of N_2 and CO_2 from ammonia oxidation compared to what happens at atmospheric pressure. This is a positive outcome for the use of ammonia as a fuel in pressure applications such as turbines. However, the N_2O concentration in the exhaust gases is significantly higher than that in pure NH_3 oxidation, which may be a drawback.

The onset of both NH_3 and CH_4 oxidation occurs at higher temperatures for reducing and stoichiometric conditions than for oxidizing conditions for all the pressures considered, indicating the importance of oxygen stoichiometry for ammonia conversion. In addition, working at higher oxygen excess ratios minimizes HCN production.

Compared to the oxidation of pure ammonia, the presence of CH_4 acts to shift ammonia conversion to lower temperatures, up to 300 K under certain conditions.

Pressure is seen to have an important influence on both the NH_3 and CH_4 oxidation regimes in the mixture, shifting them to lower temperatures as the pressure increases. However, the influence of pressure is seen to be significantly more important at low pressures compared to high pressures, and, at the same time, this influence is lower at higher CH_4/NH_3 ratios.

The production of OH, CH_3, and HCO species promotes the NH_3 and CH_4 consumption and, on the counterpart, the inhibition of NH_3 and CH_4 combustion is favored by reactions that produce HO_2, H_2O, and O_2 species, under the studied conditions.

The mechanism compiled from the literature and updated in the present work, used to carry out the simulations, is able to describe well the conversion of both NH_3 and CH_4 under almost all of the studied conditions. Nevertheless, discrepancies, mainly in the prediction of NH_3, NO, N_2, N_2O, and CO_2 under certain

https://doi.org/10.1021/acs.energyfuels.3c03959
Energy Fuels 2024, 38, 1399−1415

experimental conditions, have been observed, with higher discrepancies between the experimental and calculated results seen for N_2O. The best agreement between experimental results and calculations is found for oxidizing conditions.

■ ASSOCIATED CONTENT

Supporting Information

The Supporting Information is available free of charge at https://pubs.acs.org/doi/10.1021/acs.energyfuels.3c03959.

Validation of kinetic mechanism; table of experimental onset reaction NH_3 and CH_4 temperatures; N_2 and NO species concentration figures; comparison of pressure and residence time effect; and N_2O species concentration rescaled figure (PDF)

Mechanism details (TXT)

Thermodynamic data listing (TXT)

■ AUTHOR INFORMATION

Corresponding Author

María U. Alzueta − *Department of Chemical and Environmental Engineering, Aragón Institute of Engineering Research (I3A), University of Zaragoza, 50018 Zaragoza, Spain;* orcid.org/0000-0003-4679-5761; Email: uxue@unizar.es

Authors

Pedro García-Ruiz − *Department of Chemical and Environmental Engineering, Aragón Institute of Engineering Research (I3A), University of Zaragoza, 50018 Zaragoza, Spain;* orcid.org/0000-0003-2800-8197

Iris Salas − *Department of Chemical and Environmental Engineering, Aragón Institute of Engineering Research (I3A), University of Zaragoza, 50018 Zaragoza, Spain*

Eva Casanova − *Department of Chemical and Environmental Engineering, Aragón Institute of Engineering Research (I3A), University of Zaragoza, 50018 Zaragoza, Spain*

Rafael Bilbao − *Department of Chemical and Environmental Engineering, Aragón Institute of Engineering Research (I3A), University of Zaragoza, 50018 Zaragoza, Spain*

Complete contact information is available at: https://pubs.acs.org/10.1021/acs.energyfuels.3c03959

Notes

The authors declare no competing financial interest.

■ ACKNOWLEDGMENTS

The authors acknowledge the funding from the Aragón Government (ref. T22_23R), cofunded by FEDER 2014-2020 "Construyendo Europa desde Aragón", to MINECO and FEDER (Projects RTI2018-098856-B-I00 and PID2021-124032OB-I00), and MINECO PRE2019-090162 for financial support.

■ REFERENCES

(1) Valera-Medina, A.; Bañares-Alcántara, R. Introduction. In *Techno-Economic Challenges Green Ammon. as an Energy Vector*; Elsevier, 2021; pp 1−14.

(2) Tang, H.; Yang, C.; Wang, G.; Guiberti, T. F.; Magnotti, G. Raman Spectroscopy for Quantitative Measurements of Temperature and Major Species in High-Pressure Non-Premixed $NH_3/H_2/N_2$ Counterflow Flames. *Combust. Flame* **2022**, *237*, No. 111840.

(3) Colom-Díaz, J. M.; Millera; Bilbao, R.; Alzueta, M. U. High Pressure Study of H_2 Oxidation and its Interaction with NO. *Int. J. Hydrogen Energy* **2019**, *44*, 6325−6332.

(4) Yang, S. J.; Jung, H.; Kim, T.; Park, C. R. Recent Advances in Hydrogen Storage Technologies Based on Nanoporous Carbon Materials. *Prog. Nat. Sci. Mater. Int.* **2012**, *22*, 631−638.

(5) Duynslaegher, C.; Contino, F.; Vandooren, J.; Jeanmart, H. Modeling of Ammonia Combustion at Low Pressure. *Combust. Flame* **2012**, *159*, 2799−2805.

(6) Okafor, E. C.; Naito, Y.; Colson, S.; Ichikawa, A.; Kudo, T.; Hayakawa, A.; Kobayashi, H. Experimental and Numerical Study of the Laminar Burning Velocity of CH_4−NH_3−Air Premixed Flames. *Combust. Flame* **2018**, *187*, 185−198.

(7) Valera-Medina, A.; Amer-Hatem, F.; Azad, A. K.; Dedoussi, I. C.; De Joannon, M.; Fernandes, R. X.; Glarborg, P.; Hashemi, H.; He, X.; Mashruk, S.; McGowan, J.; Mounaim-Rouselle, C.; Ortiz-Prado, A.; Ortiz-Valera, A.; Rossetti, I.; Shu, B.; Yehia, M.; Xiao, H.; Costa, M. Review on Ammonia as a Potential Fuel: From Synthesis to Economics. *Energy Fuels* **2021**, *35*, 6964−7029.

(8) Valera-Medina, A.; Marsh, R.; Runyon, J.; Pugh, D.; Beasley, P.; Hughes, T.; Bowen, P. Ammonia−Methane Combustion in Tangential Swirl Burners for Gas Turbine Power Generation. *Appl. Energy* **2017**, *185*, 1362−1371.

(9) Valera-Medina, A.; Xiao, H.; Owen-Jones, M.; David, W. I. F.; Bowen, P. J. Ammonia for Power. *Prog. Energy Combust. Sci.* **2018**, *69*, 63−102.

(10) Kobayashi, H.; Hayakawa, A.; Somarathne, K. D. K. A.; Okafor, E. C. Science and Technology of Ammonia Combustion. *Proc. Combust. Inst.* **2019**, *37*, 109−133.

(11) Shu, B.; Vallabhuni, S. K.; He, X.; Issayev, G.; Moshammer, K.; Farooq, A.; Fernandes, R. X. A Shock Tube and Modeling Study on the Autoignition Properties of Ammonia at Intermediate Temperatures. *Proc. Combust. Inst.* **2019**, *37*, 205−211.

(12) Alzueta, M. U.; Abián, M.; Elvira, I.; Mercader, V. D.; Sieso, L. Unraveling the NO Reduction Mechanisms Occurring during the Combustion of NH_3/CH_4 Mixtures. *Combust. Flame* **2023**, *257*, No. 112531.

(13) Alzueta, M. U.; Ara, L.; Mercader, V. D.; Delogu, M.; Bilbao, R. Interaction of NH_3 and NO under Combustion Conditions. Experimental Flow Reactor Study and Kinetic Modeling Simulation. *Combust. Flame* **2022**, *235*, No. 111691.

(14) Okafor, E. C.; Somarathne, K. D. K. A.; Ratthanan, R.; Hayakawa, A.; Kudo, T.; Kurata, O.; Iki, N.; Tsujimura, T.; Furutani, H.; Kobayashi, H. Control of NO_x and Other Emissions in Micro Gas Turbine Combustors Fuelled with Mixtures of Methane and Ammonia. *Combust. Flame* **2020**, *211*, 406−416.

(15) Hayakawa, A.; Goto, T.; Mimoto, R.; Arakawa, Y.; Kudo, T.; Kobayashi, H. Laminar Burning Velocity and Markstein Length of Ammonia/Air Premixed Flames at Various Pressures. *Fuel* **2015**, *159*, 98−106.

(16) Okafor, E. C.; Naito, Y.; Colson, S.; Ichikawa, A.; Kudo, T.; Hayakawa, A.; Kobayashi, H. Measurement and Modelling of the Laminar Burning Velocity of Methane-Ammonia-Air Flames at High Pressures Using a Reduced Reaction Mechanism. *Combust. Flame* **2019**, *204*, 162−175.

(17) Alzueta, M. U.; Glarborg, P.; Dam-Johansen, K. Low Temperature Interactions Between Hydrocarbons and Nitric Oxide. An Experimental Study. *Combust. Flame* **1997**, *109*, 25−36.

(18) Mendiara, T.; Glarborg, P. Ammonia Chemistry in Oxy-Fuel Combustion of Methane. *Combust. Flame* **2009**, *156*, 1937−1949.

(19) Sun, Z.; Xu, J.; Su, S.; Qing, M.; Wang, L.; Cui, X.; Mostafa, M. E.; Zhang, C.; Hu, S.; Wang, Y.; Xiang, J. Formation and Reduction of NO from the Oxidation of NH_3/CH_4 with High Concentration of H_2O. *Fuel* **2019**, *247*, 19−25.

(20) Sun, Z.; Deng, Y.; Song, S.; Yang, J.; Yuan, W.; Qi, F. Experimental and Kinetic Modeling Study of the Homogeneous Chemistry of NH_3 and NO_x with CH_4 at the Diluted Conditions. *Combust. Flame* **2022**, *243*, No. 112015.

(21) Tian, Z.; Li, Y.; Zhang, L.; Glarborg, P.; Qi, F. An Experimental and Kinetic Modeling Study of Premixed $NH_3/CH_4/O_2$/Ar Flames at Low Pressure. *Combust. Flame* **2009**, *156*, 1413−1426.
(22) Li, B.; He, Y.; Li, Z.; Konnov, A. A. Measurements of NO Concentration in NH_3-Doped CH_4 + Air Flames Using Saturated Laser-Induced Fluorescence and Probe Sampling. *Combust. Flame* **2013**, *160*, 40−46.
(23) Valera-Medina, A.; Morris, S.; Runyon, J.; Pugh, D. G.; Marsh, R.; Beasley, P.; Hughes, T. Ammonia, Methane and Hydrogen for Gas Turbines. *Energy Procedia* **2015**, *75*, 118−123.
(24) An, Z.; Zhang, M.; Zhang, W.; Mao, R.; Wei, X.; Wang, J.; Huang, Z.; Tan, H. Emission Prediction and Analysis on CH_4/NH_3/Air Swirl Flames with LES-FGM Method. *Fuel* **2021**, *304*, No. 121370.
(25) Jójka, J.; Ślefarski, R. Dimensionally Reduced Modeling of Nitric Oxide Formation for Premixed Methane-Air Flames with Ammonia Content. *Fuel* **2018**, *217*, 98−105.
(26) Han, X.; Wang, Z.; Costa, M.; Sun, Z.; He, Y.; Cen, K. Experimental and Kinetic Modeling Study of Laminar Burning Velocities of NH_3/Air, NH_3/H_2/Air, NH_3/CO/Air and NH_3/CH_4/Air Premixed Flames. *Combust. Flame* **2019**, *206*, 214−226.
(27) Barbas, M.; Costa, M.; Vranckx, S.; Fernandes, R. X. Experimental and Chemical Kinetic Study of CO and NO Formation in Oxy-Methane Premixed Laminar Flames Doped with NH_3. *Combust. Flame* **2015**, *162*, 1294−1303.
(28) Ramos, C. F.; Rocha, R. C.; Oliveira, P. M. R.; Costa, M.; Bai, X. S. Experimental and Kinetic Modelling Investigation on NO, CO and NH_3 Emissions from NH_3/CH_4/Air Premixed Flames. *Fuel* **2019**, *254*, No. 115693.
(29) Liu, S.; Zou, C.; Song, Y.; Cheng, S.; Lin, Q. Experimental and Numerical Study of Laminar Flame Speeds of CH_4/NH_3 Mixtures under Oxy-Fuel Combustion. *Energy* **2019**, *175*, 250−258.
(30) Rocha, R. C.; Ramos, C. F.; Costa, M.; Bai, X. S. Combustion of NH_3/CH_4/Air and NH_3/H_2/Air Mixtures in a Porous Burner: Experiments and Kinetic Modeling. *Energy Fuels* **2019**, *33*, 12767−12780.
(31) Tang, G.; Jin, P.; Bao, Y.; Chai, W. S.; Zhou, L. Experimental Investigation of Premixed Combustion Limits of Hydrogen and Methane Additives in Ammonia. *Int. J. Hydrogen Energy* **2021**, *46*, 20765−20776.
(32) Zhang, M.; An, Z.; Wei, X.; Wang, J.; Huang, Z.; Tan, H. Emission Analysis of the CH_4/NH_3/Air Co-Firing Fuels in a Model Combustor. *Fuel* **2021**, *291*, No. 120135.
(33) Zhang, M.; Wei, X.; Wang, J.; Huang, Z.; Tan, H. The Blow-off and Transient Characteristics of Co-Firing Ammonia/Methane Fuels in a Swirl Combustor. *Proc. Combust. Inst.* **2021**, *38*, 5859−5868.
(34) Somarathne, K. D. K. A.; Okafor, E. C.; Sugawara, D.; Hayakawa, A.; Kobayashi, H. Effects of OH Concentration and Temperature on NO Emission Characteristics of Turbulent Non-Premixed CH_4/NH_3/Air Flames in a Two-Stage Gas Turbine like Combustor at High Pressure. *Proc. Combust. Inst.* **2021**, *38*, 5163−5170.
(35) Xiao, H.; Howard, M.; Valera-Medina, A.; Dooley, S.; Bowen, P. J. Study on Reduced Chemical Mechanisms of Ammonia/Methane Combustion Under Gas Turbine Conditions. *Energy Fuels* **2016**, *30*, 8701−8710.
(36) Xiao, H.; Valera-Medina, A.; Marsh, R.; Bowen, P. J. Numerical Study Assessing Various Ammonia/Methane Reaction Models for Use under Gas Turbine Conditions. *Fuel* **2017**, *196*, 344−351.
(37) Kurata, O.; Iki, N.; Matsunuma, T.; Inoue, T.; Tsujimura, T.; Furutani, H.; Kobayashi, H.; Hayakawa, A. Performances and Emission Characteristics of NH_3-Air and NH_3-CH_4-Air Combustion Gas-Turbine Power Generations. *Proc. Combust. Inst.* **2017**, *36*, 3351−3359.
(38) Kurata, O.; Iki, N.; Inoue, T.; Matsunuma, T.; Tsujimura, T.; Furutani, H.; Kawano, M.; Arai, K.; Okafor, E. C.; Hayakawa, A.; Kobayashi, H. Development of a Wide Range-Operable, Rich-Lean Low-NO_x Combustor for NH_3 Fuel Gas-Turbine Power Generation. *Proc. Combust. Inst.* **2019**, *37*, 4587−4595.
(39) Xiao, H.; Valera-Medina, A.; Bowen, P. J. Study on Premixed Combustion Characteristics of Co-Firing Ammonia/Methane Fuels. *Energy* **2017**, *140*, 125−135.
(40) Li, S.; Zhang, S.; Zhou, H.; Ren, Z. Analysis of Air-Staged Combustion of NH_3/CH_4 Mixture with Low NO_x Emission at Gas Turbine Conditions in Model Combustors. *Fuel* **2019**, *23*, 50−59.
(41) Li, R.; Konnov, A. A.; He, G.; Qin, F.; Zhang, D. Chemical Mechanism Development and Reduction for Combustion of $NH_3/H_2/CH_4$ Mixtures. *Fuel* **2019**, *257*, No. 116059.
(42) Zhao, Z.; Li, X.; Zhang, Z.; Zha, X.; Chen, Y.; Gao, G.; Wu, F.; Luo, C.; Zhang, L. Combustion Regimes and Fuel-NO Mechanism of CH_4/NH_3 Jet Diffusion Flames in Hot O_2/CO_2 Co-Flow. *Fuel Process. Technol.* **2022**, *229*, No. 107173.
(43) Dai, L.; Gersen, S.; Glarborg, P.; Mokhov, A.; Levinsky, H. Autoignition Studies of NH_3/CH_4 Mixtures at High Pressure. *Combust. Flame* **2020**, *218*, 19−26.
(44) Alzueta, M. U.; Salas, I.; Hashemi, H.; Glarborg, P. CO Assisted NH_3 Oxidation. *Combust. Flame* **2023**, *257*, No. 112438.
(45) Alzueta, M. U.; Giménez-López, J.; Mercader, V. D.; Bilbao, R. Conversion of NH_3 and NH_3-NO Mixtures in a CO_2 Atmosphere. A Parametric Study. *Fuel* **2022**, *327*, No. 125133.
(46) Alzueta, M. U.; Mercader, V. D.; Giménez-López, J.; Bilbao, R. NH_3 Conversion and NO Reduction by NH_3 in N_2/Ar and CO_2 Atmospheres. *Fuel* **2023**, *353*, No. 129212.
(47) Somarathne, K. D. K. A.; Hatakeyama, S.; Hayakawa, A.; Kobayashi, H. Numerical Study of a Low Emission Gas Turbine Like Combustor for Turbulent Ammonia/Air Premixed Swirl Flames with a Secondary Air Injection at High Pressure. *Int. J. Hydrogen Energy* **2017**, *42*, 27388−27399.
(48) Ichikawa, A.; Naito, Y.; Hayakawa, A.; Kudo, T.; Kobayashi, H. Burning Velocity and Flame Structure of CH_4/NH_3/Air Turbulent Premixed Flames at High Pressure. *Int. J. Hydrogen Energy* **2019**, *44*, 6991−6999.
(49) Liu, J.; Zou, C.; Luo, J. Experimental and Modeling Study on the Ignition Delay Times of Ammonia/Methane Mixtures at High Dilution and High Temperatures. *Proc. Combust. Inst.* **2023**, *39*, 4399−4407.
(50) Wang, S.; Wang, Z.; Chen, C.; Elbaz, A. M.; Sun, Z.; Roberts, W. L. Applying Heat Flux Method to Laminar Burning Velocity Measurements of NH_3/CH_4/Air at Elevated Pressures and Kinetic Modeling Study. *Combust. Flame* **2022**, *236*, No. 111788.
(51) Marrodán, L.; Royo, E.; Millera, Á.; Bilbao, R.; Alzueta, M. U. High Pressure Oxidation of Dimethoxymethane. *Energy Fuels* **2015**, *29*, 3507−3517.
(52) Colom-Díaz, J. M.; Abián, M.; Millera; Bilbao, R.; Alzueta, M. U. Influence of Pressure on H_2S Oxidation. Experiments and Kinetic Modeling. *Fuel* **2019**, *25*, No. 116145.
(53) García-Ruiz, P.; Uruén, M.; Abián, M.; Alzueta, M. U. High Pressure Ammonia Oxidation in a Flow Reactor. *Fuel* **2023**, *348*, No. 128302.
(54) Glarborg, P.; Miller, J. A.; Ruscic, B.; Klippenstein, S. J. Modeling Nitrogen Chemistry in Combustion. *Prog. Energy Combust. Sci.* **2018**, *67*, 31−68.
(55) Stagni, A.; Cavallotti, C.; Arunthanayothin, S.; Song, Y.; Herbinet, O.; Battin-Leclerc, F.; Faravelli, T. An Experimental, Theoretical and Kinetic-Modeling Study of the Gas-Phase Oxidation of Ammonia. *React. Chem. Eng.* **2020**, *5*, 696−711.
(56) Alzueta, M. U.; Guerrero, M.; Millera, Á.; Marshall, P.; Glarborg, P. Experimental and Kinetic Modeling Study of Oxidation of Acetonitrile. *Proc. Combust. Inst.* **2021**, *38*, 575−583.
(57) Glarborg, P.; Andreasen, C. S.; Hashemi, H.; Qian, R.; Marshall, P. Oxidation of Methylamine. *Int. J. Chem. Kinet.* **2020**, *52*, 893−906.
(58) Marrodán, L.; Pérez, T.; Alzueta, M. U. Conversion of Methylamine in a Flow Reactor and Its Interaction with NO. *Combust. Flame* **2024**, *259*, No. 113130.
(59) Burke, M. P.; Klippenstein, S. J. Ephemeral Collision Complexes Mediate Chemically Termolecular Transformations that Affect System Chemistry. *Nat. Chem.* **2017**, *9*, 1078−1082.
(60) Klippenstein, S. J.; Sivaramakrishnan, R.; Burke, U.; Somers, K. P.; Curran, H. J.; Cai, L.; Pitsch, H.; Pelucchi, M.; Faravelli, T.; Glarborg, P. HE_2 + HE_2: High Level Theory and the Role of Singlet Channels. *Combust. Flame* **2022**, *243*, No. 111975.

https://doi.org/10.1021/acs.energyfuels.3c03959
Energy Fuels 2024, 38, 1399−1415

(61) Marshall, P.; Rawling, G.; Glarborg, P. New Reactions of Diazene and Related Species for Modelling Combustion of Amine Fuels. *Mol. Phys.* **2021**, *119*, 1−28.
(62) Glarborg, P.; Hashemi, H.; Cheskis, S.; Jasper, A. W. On the Rate Constant for NH_2+HO_2 and Third-Body Collision Efficiencies for NH_2 + H(+M) and NH_2 + NH_2(+M). *J. Phys. Chem. A* **2021**, *125*, 1505−1516.
(63) Glarborg, P.; Hashemi, H.; Marshall, P. Challenges in Kinetic Modeling of Ammonia Pyrolysis. *Fuel Commun.* **2022**, *10*, No. 100049.
(64) Glarborg, P. The NH_3/NO_2/O_2 System: Constraining Key Steps in Ammonia Ignition and N_2O Formation. *Combust. Flame* **2023**, *257*, No. 112311.
(65) Klippenstein, S. J.; Glarborg, P. Theoretical Kinetics Predictions for NH_2 + HO_2. *Combust. Flame* **2022**, *236*, No. 111787.
(66) Stagni, A.; Cavallotti, C. H-Abstractions by O_2, NO_2, NH_2, and HO_2 from H_2NO: Theoretical Study and Implications for Ammonia Low-Temperature Kinetics. *Proc. Combust. Inst.* **2023**, *39*, 633−641.
(67) Cobos, C. J.; Glarborg, P.; Marshall, P.; Troe, J. Re-Evaluation of Rate Constants for the Reaction N_2H_4 (+M) ⇄ NH_2 + NH_2 (+M). *Combust. Flame* **2023**, *257*, No. 112374.
(68) Gao, Y.; Alecu, I. M.; Hashemi, H.; Glarborg, P.; Marshall, P. Reactions of Hydrazine with the Amidogen Radical and Atomic Hydrogen. *Proc. Combust. Inst.* **2023**, *39*, 571−579.
(69) Marrodán, L.; Arnal, Á. J.; Millera, Á.; Bilbao, R.; Alzueta, M. U. The Inhibiting Effect of NO Addition on Dimethyl Ether High-Pressure Oxidation. *Combust. Flame* **2018**, *197*, 1−10.
(70) Marrodán, L.; Berdusán, L.; Aranda, V.; Millera, Á.; Bilbao, R.; Alzueta, M. U. Influence of Dimethyl Ether Addition on the Oxidation of Acetylene in the Absence and Presence of NO. *Fuel* **2016**, *183*, 1−8.
(71) Marrodán, L.; Millera, Á.; Bilbao, R.; Alzueta, M. U. High-Pressure Study of Methyl Formate Oxidation and Its Interaction with NO. *Energy Fuels* **2014**, *28*, 6107−6115.
(72) Marrodán, L.; Arnal, Á. J.; Millera, Á.; Bilbao, R.; Alzueta, M. U. High-Pressure Ethanol Oxidation and Its Interaction with NO. *Fuel* **2018**, *223*, 394−400.
(73) Glarborg, P.; Alzueta, M. U.; Dam-Johansen, K. Kinetic Modeling of Hydrocarbon/Nitric Oxide Interactions in a Flow Reactor. *Combust. Flame* **1998**, *115*, 1−27.
(74) Rasmussen, C. L.; Hansen, J.; Marshall, P.; Glarborg, P. Experimental Measurements and Kinetic Modeling of CO/H_2/O_2/NO_x Conversion at High Pressure. *Int. J. Chem. Kinet.* **2008**, *40*, 454−480.
(75) Rasmussen, C. L.; Rasmussen, A. E.; Glarborg, P. Sensitizing Effects of NO_x on CH_4 Oxidation at High Pressure. *Combust. Flame* **2008**, *154*, 529−545.
(76) Rasmussen, C. L.; Wassard, K. H.; Dam-Johansen, K.; Glarborg, P. Methanol Oxidation in a Flow Reactor: Implications for the Branching Ratio of the CH_3OH + OH Reaction. *Int. J. Chem. Kinet.* **2008**, *40*, 423−441.
(77) Rasmussen, C. L.; Jakobsen, J. G.; Glarborg, P. Experimental Measurements and Kinetic Modeling of CH_4/O_2 and CH_4/C_2H_6/O_2 Conversion at High Pressure. *Int. J. Chem. Kinet.* **2008**, *40*, 778−807.
(78) Giménez-López, J.; Rasmussen, C. T.; Hashemi, H.; Alzueta, M. U.; Gao, Y.; Marshall, P.; Goldsmith, C. F.; Glarborg, P. Experimental and Kinetic Modeling Study of C_2H_2 Oxidation at High Pressure. *Int. J. Chem. Kinet.* **2016**, *48*, 724−738.
(79) Alzueta, M. U.; Borruey, M.; Callejas, A.; Millera, A.; Bilbao, R. An Experimental and Modeling Study of the Oxidation of Acetylene in a Flow Reactor. *Combust. Flame* **2008**, *152*, 377−386.
(80) Alzueta, M. U.; Muro, J.; Bilbao, R.; Glarborg, P. Oxidation of Dimethyl Ether and Its Interaction with Nitrogen Oxides. *Isr. J. Chem.* **1999**, *39*, 73−86.
(81) Burke, U.; Somers, K. P.; O'Toole, P.; Zinner, C. M.; Marquet, N.; Bourque, G.; Petersen, E. L.; Metcalfe, W. K.; Serinyel, Z.; Curran, H. J. An Ignition Delay and Kinetic Modeling Study of Methane, Dimethyl Ether, and Their Mixtures at High Pressures. *Combust. Flame* **2015**, *162*, 315−330.
(82) Zhao, Z.; Chaos, M.; Kazakov, A.; Dryer, F. L. Thermal Decomposition Reaction and a Comprehensive Kinetic Model of Dimethyl Ether. *Int. J. Chem. Kinet.* **2008**, *40*, 1−18.
(83) Marshall, P.; Glarborg, P. Ab Initio and Kinetic Modeling Studies of Formic Acid Oxidation. *Proc. Combust. Inst.* **2015**, *35*, 153−160.
(84) Ansys Chemkin-Pro 17.2. Chemkin ANSYS Reaction Design. San Diego 2016 - Chemical Kinetic simulation software. https://www.ansys.com/products/fluids/ansys-chemkin-pro (accessed June 21, 2023).
(85) Song, Y.; Hashemi, H.; Christensen, J. M.; Zou, C.; Marshall, P.; Glarborg, P. Ammonia Oxidation at High Pressure and Intermediate Temperatures. *Fuel* **2016**, *181*, 358−365.
(86) Sumathi, R.; Peyerimhoff, S. D. A Quantum Statistical Analysis of the Rate Constant for the HO_2 + NH_2 Reaction. *Chem. Phys. Lett.* **1996**, *263*, 742−748.
(87) Marrodán, L.; Millera, Á.; Bilbao, R.; Alzueta, M. U. An Experimental and Modeling Study of Acetylene-Dimethyl Ether Mixtures Oxidation at High-Pressure. *Fuel* **2022**, *327*, No. 125143.
(88) Kristensen, P. G.; Glarborg, P.; Dam-Johansen, K. Nitrogen Chemistry during Burnout in Fuel-Staged Combustion. *Combust. Flame* **1996**, *107*, 211−222.
(89) Wargadalam, V. J.; Löffler, G.; Winter, F.; Hofbauer, H. Homogeneous Formation of NO and N_2O from the Oxidation of HCN and NH_3 at 600 - 1000°C. *Combust. Flame* **2000**, *120*, 465−478.
(90) https://www.epa.gov/ghgemissions/understanding-global-warming-potentials#:~:text=Nitrous%20Oxide%20 (N2O,than %20100%20years%2C%20on%20average. EPA. October 2023.